Laboratory Plasma Wave Experiments

by

F. W. Crawford

April 1968

SU-IPR Report No. 236

Prepared under
NASA Grants NGR 05-020-077
and NGR 05-020-176

INSTITUTE FOR PLASMA RESEARCH
STANFORD UNIVERSITY, STANFORD, CALIFORNIA

LABORATORY PLASMA WAVE EXPERIMENTS

by

F. W. Crawford

NASA Grants NGR 05-020-077
and NGR 05-020-176

SU-IPR Report No. 236

April 1968

[Invited paper to be presented at: NATO Advanced Study Institute on Plasma Waves in Space and in the Laboratory, Røros, Norway, April 1968.]

Institute for Plasma Research
Stanford University
Stanford, California

CONTENTS

LIST OF FIGURES

LABORATORY PLASMA WAVE EXPERIMENTS

by

F. W. Crawford

Institute for Plasma Research
Stanford University
Stanford, California

ABSTRACT

Small-signal plasma wave propagation is normally analyzed in one of three limits. In the first, the plasma is assumed to be cold. In the next higher approximation, thermal motions are taken into account via transport equations. In the third, the Boltzmann equation is employed. Each approach has its postulated domain of validity which can ultimately be checked only by experiment. This paper outlines briefly the various basic wave modes predicted in the three approximations, and describes a few of the significant laboratory plasma wave experiments that have tested the applicability of each model. It is concluded that the major predictions of cold plasma theory, macroscopic theory, and the full microscopic theory have all been supported by experiments on near-Maxwellian plasmas. The success of the small-signal theory provides the foundation on which extensions to nonlinear plasma behavior can be built with confidence. The next phase of experimental effort should be directed to detailed verification of such nonlinear theory.

1. INTRODUCTION

Plasma wave phenomena occupy a central place in almost all areas of plasma physics. They owe their importance to the fact that the response of a linear physical system to a signal can often be expressed in terms of elementary waves by use of suitable transforms in time and space. It follows that an understanding of characteristic wave properties, for example, knowledge of whether the various modes are growing or attenuating, is fundamental to prediction of plasma behavior. Naturally, in a practical situation, such complicating factors as nonlinearity, plasma inhomogeneity, and the presence of boundaries, hinder the application of simple wave theory. Even where these factors can be taken into account, the complexity of the mathematical results often defies economical solution by numerical methods. In such circumstances, recourse must always be made to comparison with experiment, to determine how simplified a physical model may be used to predict results with what we arbitrarily decide is sufficient precision.

A logical approach to the laying and testing of the foundations of plasma wave theory might be to prepare a series of experimental plasmas suitable for checking analyses of models of progressively increasing complexity. For example, an effectively infinite low temperature plasma might be used for checking the modifying effects of cold plasma on free space electromagnetic wave propagation. A magnetic field could then be added. New modes would be observed, and the plasma temperature could be raised to determine its influence on the propagation. This is not, of course, the line along which research on plasma waves has always proceeded, but is the way in which this paper will be presented. In what follows, we shall attempt to review very briefly the numerous areas in which progress in reconciling theory with experiment has been made in the laboratory. The literature is vast, and several hundred references would have to be cited in any detailed description of the developments and results. We shall confine ourselves to a few specimen comparisons with theory, chosen without regard to priority. A fair proportion of these have been taken from Stanford work because of its ready accessibility to the author.

To keep the paper to a reasonable length, only stable Maxwellian plasmas will be discussed. This ignores completely the extensive literature on instabilities, much of which has led to substantial agreement between theoretical and experimental results. We shall further confine the discussion almost exclusively to wave modes in which electrons play the dominant role. This excludes many low-frequency waves for which the significant frequencies fall near the ion cyclotron, ion plasma, or lower hybrid frequencies. Again, this leaves out many results showing strong experimental support for theory. Finally, our discussion will be limited to the common laboratory conditions of nonrelativistic plasmas.

The plan of the paper is as follows. Section 2 sketches the basic theory of plasma waves, and distinguishes between the various mathematical approaches taken, on a basis of their treatment of thermal motions. The resulting descriptions of wave modes can then be divided in a rather different manner. They will be separated according to whether they are transverse (electromagnetic), or longitudinal (electrostatic). Section 3 deals with transverse waves, while Sections 4 and 5 treat longitudinal waves with zero and nonzero applied magnetic fields, respectively. Section 6 concludes the paper with some comments on the work, and some suggestions as to where future progress may lead.

2. BASIC THEORY OF PROPAGATION IN INFINITE PLASMAS

The analysis of plasma wave propagation is now highly refined, and it will only be necessary to point out one or two of the salient features here. For information on the basic derivations, the reader should refer to the extensive literature currently available.[1-12] The problem reduces to combining the equations of charged particle motion with Maxwell's equations. For plasma, the latter may be stated as

$$\nabla \times \underset{\sim}{E} = -\frac{\partial \underset{\sim}{B}}{\partial t} , \quad \nabla \times \underset{\sim}{H} = \underset{\sim}{J} + \frac{\partial \underset{\sim}{D}}{\partial t} , \quad \nabla \cdot \underset{\sim}{D} = \rho , \quad \nabla \cdot \underset{\sim}{B} = 0 , \tag{1}$$

where $\underset{\sim}{J}$ is the current density and ρ is the volume charge density. In addition, we have the constitutive relations,

$$\underset{\sim}{D} = \epsilon_0 \underset{\sim}{E} , \quad \underset{\sim}{B} = \mu_0 \underset{\sim}{H} , \tag{2}$$

where ϵ_0 and μ_0 are the permittivity and permeability of free space. All other quantities are functions of the space variable, $\underset{\sim}{r}$, and time, t. Determination of an explicit form for $\underset{\sim}{J}$ or ρ requires a description of the particle motions in terms of the field quantities $\underset{\sim}{E}$, $\underset{\sim}{D}$, $\underset{\sim}{B}$, and $\underset{\sim}{H}$.

At this point, the first major approximation is usually made. The equations of motion, which are generally nonlinear, are linearized, and from there on the analysis proceeds in perturbation form. It follows that any predictions resulting from it will be valid only for small signals, where the limiting amplitudes which can be regarded as small can be established from higher-order theory, or by experiment. We shall return to this point again in Section 6. The use of the small-signal linear approximation opens the way to introduction of the powerful methods of transform analysis. If we define the time-Fourier transforms,

$$\underset{\sim}{E}(\omega) = \int_{-\infty}^{\infty} \underset{\sim}{E}(t) \exp(-j\omega t)\, dt , \quad \underset{\sim}{E}(t) = \frac{1}{2\pi} \int_{-\infty}^{\infty} \underset{\sim}{E}(\omega) \exp(j\omega t)\, d\omega , \tag{3}$$

then the quantities in Eq. (1) become functions of $(\underset{\sim}{r},\omega)$. Similarly, we may define the space-Fourier transforms,

$$\underset{\sim}{E}(\underset{\sim}{k}) = \int_{-\infty}^{\infty} \underset{\sim}{E}(\underset{\sim}{r}) \exp(j\underset{\sim}{k} \cdot \underset{\sim}{r})\, d\underset{\sim}{k}\ , \quad \underset{\sim}{E}(\underset{\sim}{r}) = \frac{1}{2\pi} \int_{-\infty}^{\infty} \underset{\sim}{E}(\underset{\sim}{k}) \exp(-j\underset{\sim}{k} \cdot \underset{\sim}{r})\, d\underset{\sim}{r} \tag{4}$$

so that the quantities become functions of $(\underset{\sim}{k},\omega)$.

Application of Eqs. (3) and (4) implies that the various quantities can be considered as a superposition of elementary plane waves propagating as $\exp j(\omega t - \underset{\sim}{k} \cdot \underset{\sim}{r})$. This requires plasma homogeneity in any coordinate directions along which spatial transforms are taken. It implies that the plasma must be infinite, or at least very large compared with a wavelength, though some problems can be handled with finite transforms. Implicit in this, is that solution of bounded plasma problems is effectively limited to those whose geometry permits separation of the wave equation.

The apparently straightforward steps of Eqs. (3) and (4) conceal many pitfalls and subtleties. They ultimately lead to dispersion relations of the form $D(\underset{\sim}{k},\omega) = 0$, which describe the characteristics of eternal plane waves. In many physical problems, it is only possible to understand and predict the plasma behavior correctly if a superposition of waves is considered, and the phenomenon of interest is treated as an initial value problem. In such a situation, Laplace analysis in time is required. Examples are the precise treatment of Landau damping,[3] stability analysis,[13] asymptotic time response,[14] and the determination of limiting conditions on cyclotron harmonic wave propagation perpendicular to a static magnetic field.[15] These questions will not be dealt with here. We shall restrict ourselves to the derivation and verification of dispersion relations.

One of the major benefits conferred by transform methods is that they allow the plasma to be characterized by an equivalent relative permittivity, $\overleftrightarrow{\underset{\sim}{\epsilon}}_p(\underset{\sim}{k}, \omega)$, which is in general a tensor quantity. Equation (1) then reduces to

$$\underset{\sim}{k} \times \underset{\sim}{E} = \omega\mu_0\underset{\sim}{H}\ , \quad \underset{\sim}{k} \times \underset{\sim}{H} = -\omega\epsilon_0\overleftrightarrow{\underset{\sim}{\epsilon}}_p \cdot \underset{\sim}{E}\ , \quad \underset{\sim}{k} \cdot \overleftrightarrow{\underset{\sim}{\epsilon}}_p \cdot \underset{\sim}{E} = 0\ , \quad \underset{\sim}{k} \cdot \underset{\sim}{B} = 0\ , \tag{5}$$

from which the wave equation can be derived in either of the two equivalent forms,

$$\underset{\sim}{k} \times (\underset{\sim}{k} \times \underset{\sim}{E}) + \frac{\omega^2}{c^2} \overleftrightarrow{\epsilon}_p \cdot \underset{\sim}{E} = 0 = \underset{\sim}{k}(\underset{\sim}{k} \cdot \underset{\sim}{E}) - k^2 \underset{\sim}{E} + \frac{\omega^2}{c^2} \overleftrightarrow{\epsilon}_p \cdot \underset{\sim}{E} . \qquad (6)$$

Equation (6) yields three simultaneous equations for the three orthogonal components of $\underset{\sim}{E}$. For a nontrivial solution, the determinant of the coefficients must vanish. This determinantal expression is the wave dispersion relation, $D(\underset{\sim}{k}, \omega)$.

It is to be expected that judicious choice of coordinate axes, and wave propagation angles, will lead to simple forms of Eq. (6). This is so, and is the basis of our classification and description of the modes in Sections 3-5. A most important additional distinction to be made is between longitudinal waves, for which we have in Eq. (6) $\underset{\sim}{k} \times \underset{\sim}{E} \approx 0$ $(\underset{\sim}{k} \parallel \underset{\sim}{E})$, and transverse waves, for which $\underset{\sim}{k} \cdot \underset{\sim}{E} \approx 0$ $(\underset{\sim}{k} \perp \underset{\sim}{E})$. The conditions under which these approximations may be valid can be understood only from study of $\underset{\sim}{\epsilon}_p$. The form of this quantity depends on the particular analytical treatment used for the particle motions. Discussion of this topic will take up the remainder of the section.

2.1 Cold Plasma Theory.

The equation of motion chosen for charged particles of charge q, and mass m, is commonly of the form,

$$m \frac{d\underset{\sim}{v}}{dt} = q(\underset{\sim}{E} + \underset{\sim}{v} \times \underset{\sim}{B}) - \nu m \underset{\sim}{v} . \qquad (7)$$

It contains a Lorentz force term accounting for the effects of electric and magnetic fields, and a Langevin collision term to account for momentum transfer. The collision frequency, ν, is assumed to be independent of speed. For $\nu = 0$, the equivalent permittivity resulting from use of Eq. (7) is

$$\overleftrightarrow{\epsilon}_p \equiv \begin{vmatrix} \epsilon_\perp & -j\epsilon_\times & 0 \\ j\epsilon_\times & \epsilon_\perp & 0 \\ 0 & 0 & \epsilon_\parallel \end{vmatrix} , \qquad (8)$$

$$\epsilon_{\perp} = 1 - \frac{\omega_p^2}{\omega^2 - \omega_c^2}, \quad \epsilon_{\times} = \frac{\omega_p^2 \omega_c}{\omega(\omega^2 - \omega_c^2)}, \quad \epsilon_{\parallel} = 1 - \frac{\omega_p^2}{\omega^2},$$

where ion motions have been ignored. Here, ω_p and ω_c are the electron plasma and cyclotron frequencies, respectively, defined by

$$\omega_p^2 = \frac{nq^2}{\epsilon_0 m}, \quad \omega_c = \left| \frac{qB_0}{m} \right|, \tag{9}$$

and B_0 is the static magnetic field. Collisions can be taken into account by replacing m by $m(1-j\nu/\omega)$, wherever it occurs.

A useful transformation is to work in rotating coordinates. The expressions of Eq. (8) then become,

$$\overleftrightarrow{\underset{\sim}{\epsilon}}_p \equiv \begin{vmatrix} \epsilon_R & 0 & 0 \\ 0 & \epsilon_L & 0 \\ 0 & 0 & \epsilon_{\parallel} \end{vmatrix}, \tag{10}$$

$$\epsilon_R = 1 - \frac{\omega_p^2}{\omega(\omega - \omega_c)}, \quad \epsilon_L = 1 - \frac{\omega_p^2}{\omega(\omega + \omega_c)}, \quad \epsilon_{\parallel} = 1 - \frac{\omega_p^2}{\omega^2},$$

where subscripts R and L denote right- and left-hand polarized modes. The field quantities are defined by relations of the form,

$$E_R = \frac{E_x + jE_y}{2^{\frac{1}{2}}}, \quad E_L = \frac{E_x - jE_y}{2^{\frac{1}{2}}}, \tag{11}$$

and $\underset{\sim}{B}_0$ is oriented along the z-axis. The form of Eq. (10) is appropriate to electrons.

From the experimentalist's viewpoint, the most convenient modes to study are the so-called "principal" waves, which propagate purely parallel to, or exactly perpendicular to, $\underset{\sim}{B}_0$. These will be considered further here, and in Sections 3-5.

2.1.1 Principal waves along $\underset{\sim}{B}_0(\underset{\sim}{k} \parallel \underset{\sim}{B}_0)$: There are three possible solutions given by,

$$\frac{k_{\parallel}^2 c^2}{\omega^2} = 1 - \frac{\omega_p^2}{\omega(\omega - \omega_c)} , \quad \frac{k_{\parallel}^2 c^2}{\omega^2} = 1 - \frac{\omega_p^2}{\omega(\omega + \omega_c)} , \quad 0 = 1 - \frac{\omega_p^2}{\omega^2} . \tag{12}$$

The first two are right- and left-hand polarized transverse waves, respectively. The third is a longitudinal wave of arbitrary $k_{\parallel}$. It may be thought of as longitudinal oscillation at the electron plasma frequency, ω_p.

2.1.2 Principal waves across $\underset{\sim}{B}_0(\underset{\sim}{k} \perp \underset{\sim}{B}_0)$: There are two solutions given by,

$$\frac{k_{\perp}^2 c^2}{\omega^2} = 1 - \frac{\omega_p^2}{\omega^2} , \quad \frac{k_{\perp}^2 c^2}{\omega^2} = 1 - \frac{\omega_p^2(\omega^2 - \omega_p^2)}{\omega^2(\omega^2 - \omega_p^2 - \omega_c^2)} . \tag{13}$$

The first is linearly polarized, and has $\underset{\sim}{E} \parallel \underset{\sim}{B}_0$. In ionospheric terminology (but not always elsewhere!) it is known as the "ordinary" mode. It is clearly insensitive to the presence of the static magnetic field. The second has $\underset{\sim}{E} \perp \underset{\sim}{B}_0$, and is elliptically polarized in the plane perpendicular to $\underset{\sim}{B}_0$. In ionospheric terminology it is the "extraordinary" mode.

2.2 Macroscopic Theory.

The next two approaches to be discussed take account of plasma thermal motions. Both involve use of the Boltzmann equation, which is commonly written for each charged particle species as

$$\frac{\partial f}{\partial t} + \nabla_r \cdot \underset{\sim}{v} f + \frac{q}{m} (\underset{\sim}{E} + \underset{\sim}{v} \times \underset{\sim}{B}) \cdot \nabla_v f = \nu(f_0 - f) , \tag{14}$$

where $f(\underset{\sim}{r},\underset{\sim}{v},t)$ is the particle velocity distribution; f_0 is its unperturbed value, and we have

$$\rho = q \int f \, d\underset{\sim}{v} , \qquad \underset{\sim}{J} = q \int \underset{\sim}{v} f \, d\underset{\sim}{v} . \tag{15}$$

In the microscopic approach, to be dealt with in Section 2.3, Eq. (14) is used directly. The perturbation solution for f, obtained after transforming the equation, is substituted in Eq. (15). In the macroscopic approach, successive moments of the Boltzmann equation are taken with respect to velocity to obtain the following transport equations:

$$\frac{\partial n}{\partial t} + \nabla \cdot n\underset{\sim}{v} = \nu_i , \qquad nm \frac{d\underset{\sim}{v}}{dt} + \nabla p = nq(\underset{\sim}{E} + \underset{\sim}{v} \times \underset{\sim}{B}) - n\nu m\underset{\sim}{v} . \tag{16}$$

The first equation states particle continuity, and ν_i represents the ionizing collision frequency. This equation gives n (or ρ) in terms of $n\underset{\sim}{v}$ (or $\underset{\sim}{J}$). The second is similar to the equation of motion of Eq. (7) except that it contains a scalar pressure term, p, which is usually replaced by $\gamma n\kappa T$. In this last expression, γ is the compression constant for the species; κ is Boltzmann's constant, and T is the species temperature, which is invariably defined for a Maxwellian velocity distribution in the cases of interest here. The continuity equation is exact. The equation of motion is approximate, however, since it has been obtained by truncating the moment expansion, and ignoring off-diagonal terms in the more general pressure tensor.

We now have to determine what modifications are imposed on the modes discussed in Sections 2.1.1 and 2.1.2, and what new modes are predicted, due to nonzero plasma electron temperature:

2.2.1 <u>Principal waves along $\underset{\sim}{B}_0(\underset{\sim}{k} \parallel \underset{\sim}{B}_0)$</u>: It is found that, to first order, the right- and left-hand polarized waves are unaffected, but that the plasma oscillations described by Eq. (10) now become dispersive.[4] Ignoring collisions, we have for this mode

$$\omega^2 = \omega_p^2 + k_\parallel^2 \left(\frac{3\kappa T_e}{m} \right) . \tag{17}$$

If the next moment equation is derived, a correction to the circularly polarized modes can be obtained, satisfactory for low electron temperatures and magnetic fields,[8]

$$\frac{k_\parallel^2 c^2}{\omega^2} = 1 - \frac{\omega_p^2}{\omega[\omega(1-\delta) - \omega_c]}, \quad \frac{k_\parallel^2 c^2}{\omega^2} = 1 - \frac{\omega_p^2}{\omega[\omega(1-\delta) + \omega_c]}, \quad \delta = \frac{(\kappa T_e/m)}{(\omega^2/k_\parallel^2)} . \tag{18}$$

The quantity $\delta^{\frac{1}{2}}$ represents the ratio of electron thermal velocity to phase velocity of the wave, and must be small for the analysis to be valid. The two dispersion relations of Eq. (18) can also be written approximately as,

$$\frac{k_\parallel^2 c^2}{\omega^2} = \left[1 - \frac{\omega_p^2}{\omega(\omega \mp \omega_c)}\right]\left[1 - \frac{\omega_p^2}{\omega^2}\left(\frac{\kappa T_e}{mc^2}\right)\right] . \tag{19}$$

2.2.2 Principal waves across $\underset{\sim}{B}_0$ ($\underset{\sim}{k} \perp \underset{\sim}{B}_0$): The corrected forms of Eq. (13) are[8]

$$\frac{k_\perp^2 c^2}{\omega^2} = 1 - \frac{\omega_p^2}{\omega^2}\left[1 - \frac{\omega_p^2}{\omega^2}\left(\frac{\kappa T_e}{mc^2}\right)\right] ,$$

$$\frac{k_\perp^2 c^2}{\omega^2} = \left[1 - \frac{\omega_p^2(\omega^2 - \omega_p^2)}{\omega^2(\omega^2 - \omega_p^2 - \omega_c^2)}\right]\left[1 - \frac{\omega_p^2}{\omega^2}\left(\frac{\kappa T_e}{mc^2}\right)\right] . \tag{20}$$

The correction term is the same as in Eq. (19), and will be small.

2.2.3 New modes for $T_e \neq 0$: In the analysis leading to Eq. (20) an additional longitudinal mode is obtained, propagating perpendicular to the magnetic field with the dispersion relation

$$\omega^2 = \omega_p^2 + \omega_c^2 + k_\perp^2 \left(\frac{3\kappa T_e}{m}\right) . \tag{21}$$

This expression is valid within the approximation $\omega_c^2 \ll \omega_p^2$. In the limit $\omega_c \to 0$, it is clearly equivalent to Eq. (17).

It can be shown from macroscopic theory that other new modes appear for nonzero electron temperature.[3] Longitudinal ion acoustic and ion cyclotron waves are predicted, in which ion motions are effectively driven by the electron pressure term in Eq. (16). The dispersion relations are, respectively,

$$\omega^2 = \frac{\omega_{pi}^2}{\left[1 + \frac{\omega_{pi}^2}{k_{\parallel}^2}\left(\frac{m_i}{\kappa T_e}\right)\right]} , \qquad \omega^2 = \omega_{ci}^2 + k_{\perp}^2\left(\frac{\kappa T_e}{m_i}\right) , \tag{22}$$

where ω_{ci}, ω_{pi}, and m_i are the ion cyclotron frequency, plasma frequency, and mass. For $k_{\parallel}$ small, Eq. (22) reduces to

$$\frac{\omega^2}{k_{\parallel}^2} = \left(\frac{\kappa T_e}{m_i}\right) , \tag{23}$$

which is also the limiting form of the ion cyclotron wave as $\omega_{ci} \to 0$. It indicates a constant phase velocity, independent of the electron density.

2.3 Microscopic Theory.

It is probably intuitively obvious that as long as a wave is propagating at a velocity substantially above the charged particle thermal velocities, macroscopic theory will give a good approximation to its dispersion characteristics. When the phase velocity of the wave is in the thermal velocity range we might expect rather more substantial modifications, and perhaps new phenomena. The correctness of these suppositions is borne out by detailed microscopic theory. Since we are concerned with plasmas which have nonrelativistic electron temperatures, it is sufficient to reexamine only those waves already discussed which can have phase velocities small compared with the speed of light.

2.3.1 Propagation along $\underset{\sim}{B}_0$ ($\underset{\sim}{k} \parallel \underset{\sim}{B}_0$):

The first candidate in this class is the electroacoustic wave described by Eq. (17). The modified dispersion relation given by microscopic theory for this wave is,

$$0 = 1 - \frac{\omega_p^2}{k_\parallel^2}\left(\frac{m}{2\kappa T_e}\right) Z'(\xi_0) \ , \quad \xi_0 = \frac{\omega}{k_\parallel}\left(\frac{m}{2\kappa T_e}\right)^{\frac{1}{2}} , \tag{24}$$

where Z is the plasma dispersion function,[16] defined by

$$Z(\xi) = \begin{cases} \dfrac{1}{\pi^{\frac{1}{2}}} \displaystyle\int_{-\infty}^{\infty} \frac{\exp(-t^2)\, dt}{t-\xi} & (\xi_i < 0) \ , \\[2ex] \dfrac{1}{\pi^{\frac{1}{2}}} \displaystyle\int_{-\infty}^{\infty} \frac{\exp(-t^2)\, dt}{t-\xi} - i\pi^{\frac{1}{2}} \exp(-\xi^2) & (\xi_i = 0) \ , \\[2ex] \dfrac{1}{\pi^{\frac{1}{2}}} \displaystyle\int_{-\infty}^{\infty} \frac{\exp(-t^2)\, dt}{t-\xi} - 2i\pi^{\frac{1}{2}} \exp(-\xi^2) & (\xi_i > 0) \ , \end{cases} \tag{25}$$

and the subscript i denotes the imaginary part of ξ. In Eq. (24) the prime denotes differentiation with respect to the argument, and we have the useful identity

$$Z'(\xi) \equiv -2[1 + \xi Z(\xi)] \ . \tag{26}$$

The form of this dispersion relation has been treated in detail by Derfler,[17] and will be discussed in Section 4.2.

The second mode of interest is the right-hand polarized mode. For $(\omega/\omega_c) \lesssim 1$, this wave always has $(\omega/k_\parallel) < c$. It is the "whistler" mode in ionospheric terminology. The appropriate microscopic theory dispersion relation is

$$\frac{k_\parallel^2 c^2}{\omega^2} = 1 - \frac{\omega_p^2}{\omega k_\parallel}\left(\frac{m}{2\kappa T_e}\right)^{\frac{1}{2}} Z(\xi_c) \ , \quad \xi_c = \frac{\omega - \omega_c}{k_\parallel}\left(\frac{m}{\kappa T_e}\right)^{\frac{1}{2}} . \tag{27}$$

Both Eqs. (24) and (27) show collisionless damping. In the first case, it is termed "Landau" damping, and is due to the electrons traveling slightly slower than the wave phase velocity $(\omega \gtrsim k_\parallel v)$. These extract energy from the wave so as to increase their axial velocity.[3] In the second case, it is termed "cyclotron" damping, and is due to particles increasing their transverse energy at the expense of the wave. Those with velocity such that $\omega - k v_{\parallel} \approx \omega_c$ cause the damping.

2.3.2 Propagation across $\underset{\sim}{B}_0$ ($\underset{\sim}{k} \perp \underset{\sim}{B}_0$): In this case, Eq. (21) is replaced by,[3]

$$0 = 1 - \frac{\omega_p^2}{\omega_c^2} \sum_{n=1}^{\infty} \frac{2 \exp(-\lambda)\, I_n(\lambda)}{\lambda \left[\left(\frac{\omega}{n\omega_c} \right)^2 - 1 \right]}, \quad \lambda = \frac{k_\perp^2}{\omega_c^2} \left(\frac{\kappa T_e}{m} \right), \tag{28}$$

which describes longitudinal cyclotron harmonic waves. The comparison between Eq. (28) and Eqs. (24) and (27) is extremely interesting. In the latter, the correction due to taking account of thermal effects microscopically is to introduce a damping component into an otherwise purely real mode of propagation. In the case of Eq. (28), the microscopic treatment predicts new undamped modes of propagation in addition to that of Eq. (21). The characteristics of these modes will be dealt with in Section 5.2.

Although temperature effects on the transverse electromagnetic waves propagating across the magnetic field are small. One result will be quoted here that has been investigated experimentally. This is for the extraordinary mode of Eq. (13) in the vicinity of the second cyclotron harmonic. We have,[18]

$$\frac{k_\perp c}{\omega} = \left[1 - \frac{\omega_p^2(\omega^2 - \omega_p^2)}{\omega^2(\omega^2 - \omega_p^2 - \omega_c^2)} \right]^{\frac{1}{2}} \left[1 - \frac{\omega_p^2}{8\omega_c^2} \left(\frac{\kappa T_e}{mc^2} \right) \left(\frac{6\omega_c^2 - \omega_p^2}{3\omega_c^2 - \omega_p^2} \right) \frac{\omega}{\omega - 2\omega_c} \right]. \tag{29}$$

This result will be discussed further in Section 3.1.

3. TRANSVERSE WAVES

The theory discussed in Section 2 was for the case of an infinite plasma. This implies that successful experimental verification will depend on producing a plasma having a homogeneous volume of dimensions large compared with the wavelength of the plasma mode of interest. This may or may not be longer than the free space wavelength at the signal frequency, depending on the plasma mode concerned. There are, of course, checks on the theory, particularly in the cold plasma approximation, which are in the opposite sense. For example, in cavity perturbation and scattering experiments, the plasma is often small compared with a free space wavelength at the signal frequency. We shall not be concerned with such studies in this section. Some cases will be dealt with in Section 4. Here, we will confine ourselves to situations in which infinite plane wave propagation is approximated closely. For purposes of discussion, we shall classify the experiments according to whether the transmitted signal from the source is linearly- or circularly-polarized.

3.1 Linearly-Polarized.

The first wave of this type to be considered is the ordinary mode described by Eq. (13), for propagation with $\underset{\sim}{E} \| \underset{\sim}{B}_0 \perp \underset{\sim}{k}$. It has received abundant verification, and forms the basis of the commonly-used microwave interferometric diagnostic technique for measuring electron density.[8] Numerous satisfactory comparisons have been made with electron density measurements obtained by other techniques. Since microwave sources are readily available down to centimeter or even millimeter wavelengths, the essential requirement of short wavelength compared with apparatus size can be met easily. The mode is only very weakly sensitive to combined electron temperature and magnetic field effects, and no detailed verification of the microscopic theory appears to have been made.

The second mode propagating perpendicular to the magnetic field, that has been excited by a linearly-polarized source, is the extraordinary mode, whose dispersion relation was given in Eq. (13). Meservey and Schlesinger[18] have transmitted 70 GHz signals across the plasma in the Model C Stellarator, between two microwave horns, with results such as those of Fig. 1. The magnetic field was varied, and was 25 kG at $\omega = \omega_c$. It was uniform to 0.05%. The electron density was measured independently by an interferometer working in the ordinary mode. As Fig. 1(a) shows, the results agree closely with the cold plasma theory of Eq. (13). The microscopic plasma theory of Eq. (29) predicts a resonant absorption of power at $2\omega_c$ which is not suggested by either the cold plasma theory, or the macroscopic theory of Eq. (20). A good check on this theory is provided by Fig. 1(b), which shows the dispersion characteristics in the vicinity of the resonance at $(\omega/\omega_c) \approx 2$.

Finally, we consider the case of a linearly-polarized wave propagating along the magnetic field. This is effectively equivalent to the propagation of two circularly-polarized waves satisfying Eq. (12). Faraday rotation of the resultant field vectors will occur. This has been suggested as a technique for laboratory measurements of electron density[8,19] and it has been widely used in space plasma diagnostics. It has been pointed out by Bachynski and Gibbs[20], however, that since most laboratory plasmas in which such experiments can be carried out are rather lossy, the signal tends to emerge elliptically-polarized, and data reduction is thereby complicated. These authors have carried out an extensive series of measurements of rotation in a helium afterglow plasma. The results were used to obtain electron density measurements for comparison with other measurements made on the same plasma, using the right-and left-hand polarized modes separately. The results showed internal consistency, but were not compared with an independent measure of density.

3.2 <u>Circularly-Polarized</u>.

In view of the foregoing comments, it might be expected that clearer results could be obtained by exciting the two circularly-polarized waves of Eq. (12) separately. This has been attempted by numerous authors, and a comprehensive bibliography has been given by Bachynski and Gibbs[20-21] in connection with their own work. In some of the experiments, the plasma density and/or the magnetic field were pulsed, and observations were made of the various cut-offs and resonances of the two polarized modes transmitted through the plasma along the magnetic field. Another popular technique has been to use wave theory to derive the electron density from transmission measurements through a plasma of fixed length, and then to compare it with measurements made using an independent mode, for example, by ordinary mode interferometry across the discharge.

An alternative technique is illustrated in Fig. 2(a) by which interferometric measurements of right-hand polarized (whistler) propagation have been obtained. The experiments were carried out at a few GHz in the afterglow of a pulsed reflex discharge in argon, and the electron density was calibrated using an interferometer operating in the ordinary mode transverse to the column. Typical results are illustrated by Fig. 2(b). They were obtained from interferometric records combining a reference signal with that transmitted between the antennas, for different antenna spacings up to about 10 cm.

It is a feature of most of the laboratory whistler measurements reported in the literature so far that either electron/neutral or Coulomb collisions had a strong damping effect on the propagation. These have their strongest influence for $(\omega/\omega_c) \leq 1$, which is also the region where Eq. (27) predicts collisionless cyclotron damping to be important. The effect seems to have been noted previously only in the work of Mahaffey,[22] and no detailed check on the theory has appeared. Recently, the author and his colleagues have been trying to measure such damping. Some preliminary results obtained in the set-up of Fig. 2(a) are shown in Fig. 2(c), with theoretical curves computed from Eq. (27) for comparison. At the moment, the agreement is only fair. The major difficulty encountered in comparing theory with such experiments is that the attenuation is extremely sensitive to electron temperature. This is a quantity which is very difficult to measure precisely in a strong magnetic field.

4. LONGITUDINAL WAVES: ZERO MAGNETIC FIELD

The theory of longitudinal plasma waves normally invokes an additional simplifying assumption to those mentioned in Section 2. This is the "quasistatic," or "slow-wave," assumption, and is valid for[3]

$$c^2 \gg \frac{\omega^2}{k^2} |\epsilon_{pij}| \quad , \tag{30}$$

where ϵ_{pij} is the i,jth component of the equivalent plasma permittivity tensor. The assumption implies that the wave can only be strictly longitudinal if its phase velocity is small compared with the speed of light. Under these conditions, the electric field can be derived from a scalar potential, ϕ, and Poisson's equation can be written for the plasma as

$$\nabla \cdot \overleftrightarrow{\underset{\sim}{\epsilon}}_p \cdot \nabla \phi = 0, \qquad \underset{\sim}{k} \cdot \overleftrightarrow{\underset{\sim}{\epsilon}}_p \cdot \underset{\sim}{k} = 0 \ , \tag{31}$$

where the second expression has been Fourier-transformed in space. Equation (31) does not lead to dispersive propagation in an unbounded plasma, though it does, of course, predict such phenomena as the plasma frequency oscillations of Eq. (12). If the plasma is bounded, however, new modes are indicated, unrelated to the wave types discussed so far and which we shall class as "transmission line" modes. Elsewhere, they are often described as "space charge" waves.[8] These modes will be discussed in Section 4.1. In Section 4.2, we shall then discuss results on warm plasma propagation.

4.1 Cold Plasma Waves.

Before proceeding to a discussion of transmission line modes, we may comment on the simple case of dispersionless cold plasma oscillations described by Eq. (12). In practice, the macroscopic and microscopic theory corrections to this mode, expressed in Eqs. (17) and (24), will become important for plasma wavelengths less than about ten electronic Debye lengths. It is ironic that a laboratory demonstration of this most simple and fundamental case of oscillation at the plasma frequency, which was one of the first to be analyzed, is one of the most recent to be made. An interesting means by which such oscillations can be stimulated is by shock-exciting the plasma with a short (nsec) pulse. An elegant experiment of this type, performed in an inhomogeneous afterglow plasma, has been reported recently by Baldwin et al.[23]

The propagation of transmission line modes has received very intensive study over the last ten years, mainly in experiments using cylindrical low-pressure positive columns. The mechanism by which these propagate can be very easily understood from Fig. 3, in terms of the plasma equivalent permittivity concept. Consider the case of Fig. 3(a) with no static magnetic field present. The plasma permittivity $[\equiv 1 - (\omega_p^2/\omega^2)]$ is negative for $\omega^2 < \omega_p^2$, so that the plasma behaves inductively. Capacitance to a surrounding shield provides the second distributed element required for transmission line propagation.[11]

For the most simple case of a cylindrical plasma column surrounded by free space, the theoretical upper limiting frequency for propagation is $(\omega_p/2^{1/2})$. This is modified by the presence of dielectrics and an outer conductor surrounding the column, and by plasma inhomogeneity. Analyses taking these into account give good agreement with theory.[11,24,25] Some typical results are shown in Fig. 4(a), in which a parabolic density profile, $n = n_0 [1 - \alpha(r^2/a^2)]$, has been taken into account in computing the theoretical dispersion curves. The measurements were made on a mercury-vapor positive column, at about 1m Torr pressure, in apparatus generally similar to that sketched in Fig. 4(b).

A point to be noted is that accurate experimental data cannot be obtained in the region where the dispersion wave turns over and approaches its limiting value. Three factors account for this: collisions, which become important due to the low group velocity of the waves; collisionless damping, due to rf effects in the wall sheath,[25] and Landau damping at low phase velocities.

4.2 Warm Plasma - Electron Waves.

One of the most significant contributions in the area of plasma waves is the very strong support that has been given by a number of recent experiments[17,26-31] to the microscopic plasma theory from which Eq. (24) is derived. The most simple case conceptually is that of plane wave propagation, and an excellent approximation to this has been obtained in the apparatus shown in Fig. 5(a). The waves are excited in a thermal sodium plasma, produced by contact ionization at the surfaces of two heated tantalum plates, by an electrostatically screened antenna. Interferometric measurements are made using the capacitively coupled signal as a reference. The electronic Debye length, λ_D $(\equiv(\kappa T_e/m)^{1/2}/\omega_p)$, is of the order of 1 mm. Typical results are shown in Fig. 5(b) for both the real part of the wave-number, and the imaginary part due to collisionless Landau damping. The full lines represent computer solutions of Eq. (24) and the chain line represents the macroscopic theory result of Eq. (17). It will be noted that this is rather a poor approximation to the microscopic theory result, which agrees well with experiment.

The next modification of interest, after plane wave propagation has been measured, is that of propagation in a bounded plasma column. Again, the full microscopic theory extension to the cold plasma theory has been verified satisfactorily experimentally. The apparatus used by Malmberg and Wharton[26-28] to accomplish this is shown in Fig. 6(a), and some typical results are shown in Fig. 6 (b) for the real component of the wave-number. The full line represents a microscopic theory dispersion curve computed taking account of the radial density profile.[17,26-28] There is excellent agreement. Equally good agreement is indicated in Fig. 6(c) for the attenuation of the waves due to collisionless Landau damping. The full line again represents the theoretical predictions.

An interesting situation in which Landau damping might be reduced, and macroscopic theory might be applicable, is that of propagation across an inhomogeneous plasma. The usual form taken by experiments on such effects is a radially nonuniform cylindrical plasma column, to which an electric field is applied transverse to the axis. At certain frequencies, standing waves are excited which usually manifest themselves by increased absorption. A set of such resonances is illustrated in Fig. 7(a).[32,33] They were obtained in reflection from a neon afterglow plasma at 0.3 Torr. The signal frequency was fixed at 250 MHz, and the resonances were produced during decay of the plasma density (time increases to the right in Fig. 7(a)).

A detailed theory of Tonks-Dattner resonances has been carried out by Parker et al,[34] using macroscopic theory and a self-consistent dc profile for the low pressure mercury-vapor discharge column employed in their experiments. The results are shown in Fig. 7(b), for excitation in the dipole mode, and show excellent agreement with the experimental locations of the resonances. There is, however, an experimental observation which is not predicted by this theory. That is, that the resonances tend to wash out to an effective series limit when the resonance frequency, ω_r, approaches ω_{p0}, the plasma frequency at the tube axis.[34,35] This can only be predicted from full microscopic theory, including collisionless damping. This has been carried out recently by Harker,[36] and demonstrates an extremely rapid rise in the damping as ω_r tends to, or exceeds ω_{p0}.

4.3 Warm Plasma - Ion Waves.

It was mentioned in Section 2.2 that macroscopic theory predicts wave propagation phenomena involving ions, which do not appear in the cold plasma analysis. We shall discuss only one case here, for which macroscopic theory may give a good approximation under suitable experimental conditions. This is the ion acoustic wave described by Eq. (22). Its main predicted feature is plane wave propagation at the ion acoustic speed $(\kappa T_e/m_i)^{1/2}$. This has been demonstrated experimentally by Jones and Alexeff,[37] using the apparatus shown in Fig. 8(a) to obtain the results shown in Fig. 8 (b). The method involved is a group delay measurement, in which the time of flight of a pulse travelling between moveable probe antennas, in a 20cm diameter spherical discharge, is measured. The results of Fig. 8(b) are for the rare gases. The electron temperatures were $\kappa T_e \approx$ 1eV for Ne, A, Kr, Xe, and 9eV for He. The measured velocities verify the plane wave theory over a mass range of 30 to 1, and indicate isothermal compression of the electron gas.

If the electron and ion temperatures, T_e and T_i, are approximately equal, rather than widely differing, as in the discharge experiments of Jones and Alexeff for which $T_e \gg T_i$, then a microscopic analysis of ion wave propagation is required. This predicts collisionless Landau damping.[38] Ion waves propagating under these conditions were studied by Wong et al[39] in the experimental set-up shown in Fig. 9(a). In this, highly-ionized alkali metal plasma columns were produced by contact ionization at the tungsten end-plates. The dispersion characteristics were measured for ion waves excited by moveable probes located in the column. Some observations of collisionless Landau damping are shown in Fig. 9(b) for Cs and K plasmas. The theory will not be given here. It is essentially that of Fried and Gould[38] with modifications to account for axial drift. The resulting predicted values of the imaginary component of the wavenumber agree to within a few per cent with the experimental data.

In addition to the experiments in which effectively plane wave propagation of ion waves has been observed, there have been several studies of propagation along the positive column, in which boundaries play an important role. These give fair agreement with macroscopic theory,[40,41] but there are many complicating factors due to drifts and collisions, and the analysis becomes extremely involved. New modes appear,[42,40] the origins of which have only recently been elucidated.[43] The field requires further study, and a microscopic theory would probably be required to explain all of the propagation characteristics observed.

5. LONGITUDINAL WAVES: NONZERO MAGNETIC FIELD

We shall first consider the effect of a static magnetic field on the bounded plasma transmission line modes predicted by cold plasma theory, and discussed in Section 4.1. We shall then discuss warm plasma waves propagating in the cyclotron harmonic wave mode perpendicular to the magnetic field.

5.1 Cold Plasma.

The transmission line modes discussed in Section 4.1 are often termed "surface" waves, since there is no perturbation charge density within the plasma, if the unperturbed column density is uniform. The electric field lines inside and outside the plasma terminate on surface charges. If an axial magnetic field is applied, and is increased progressively from zero, the surface wave is modified and two new transmission line modes appear. These arise due to the fact that the radial and axial permittivity components, $\epsilon_\perp$ and $\epsilon_\parallel$, given by Eq. (8) can differ in sign over certain ranges of (ω/ω_p) and (ω_p/ω_c). The two basic cases are illustrated in Fig. 3(b). For the first, the phase and group velocities are in the same sense. For the second, they are opposed. The new modes are "body" waves, and show strong perturbation charge densities within the column. They can exist with the same cut-off and resonance frequencies, even if the plasma is in direct contact with a containing metallic shield, whereas for surface waves a dielectric sheath is essential to the propagation. If $\omega_c > \omega_p$, the surface wave mode disappears, and only the two body wave modes remain.

Numerous measurements have been made on body wave modes. Figures 4(b) and (c) show the set-up used, and some experimental results from the pioneer work of Trivelpiece.[11] The studies were carried out on an 8 mm diameter, low pressure mercury-vapor discharge column. In Fig. 4(c), the experimental results for $(\omega_p/\omega_c) = 1.9$ agree well with the theory for $(\omega_p/\omega_c) = 2$ in the case of the forward wave mode, but not so well for the backward wave mode. The latter is more difficult to measure, and is particularly susceptible to radial inhomogeneity of the plasma column. This is difficult to analyze within the cold plasma model, due to an awkward pole in the potential which occurs if the signal frequency equals the local upper hybrid frequency, $(\omega_p^2 + \omega_c^2)^{1/2}$, anywhere in the column. The difficulty could be relieved by use of macroscopic plasma theory, but no precise comparison seems to have been made yet between such theory and experiment.

5.2 Warm Plasma.

It was pointed out in Section 2.3 that the three major predictions peculiar to microscopic theory are Landau and cyclotron damping, and the propagation of undamped, longitudinal, cyclotron harmonic waves, perpendicular to the magnetic field. Observations of the first two effects have been described in Sections 3.2 and 4.2. We now complete the set by reference to some recent experiments on cyclotron harmonic waves. The first step should be to establish the validity of the dispersion relation expressed by Eq. (28). This has been accomplished by two methods: wave interference,[44,45] and group delay.[45-47] Figure 10 illustrates the first of these. The transfer admittance between parallel wire antennas is measured as a function of magnetic field. Apart from the major peaks near the cyclotron harmonics shown in Fig. 10(b), there is a fine structure of peaks which can be shown to be due to interference between the signal coupled capacitively between the antennas, and the propagating cyclotron harmonic wave mode. Dispersion characteristics such as those of Fig. 10(c) can be derived from records similar to that of Fig. 10(b), obtained with varying plasma density and probe spacing. The agreement indicated in Fig. 10(c) between the experimental points and the theoretical curves computed from Eq. (28) is very good over the experimental range of parameters accessible.

It is interesting to note that, in the same way that the Tonks-Dattner resonances of an inhomogeneous plasma column were observed and analyzed before the more conceptually simple plane electroacoustic wave measurements were carried out, so also was the behavior of cyclotron harmonic waves in inhomogeneous plasmas analyzed and studied experimentally prior to the plane wave studies. The first analyses of such phenomena were made by Buchsbaum and Hasegawa[48,49], to explain some early results on fine structure in the noise radiation and absorption spectra of warm magnetoplasmas. They carried out absorption measurements at a few GHz, on a plasma column contained in a microwave cavity. They interpreted the fine structure of absorption peaks, such as are shown in Fig. 11(a), in terms of standing cyclotron harmonic waves in the interior of the inhomogeneous column. Their theoretical solutions for such a situation are illustrated by the full lines in Fig. 11(b). It will be seen that there is remarkable agreement with the experimental data.

6. DISCUSSION

The most significant feature of the brief selection of results reviewed in Sections 3 to 5 is undoubtedly the very close agreement between experiment and microscopic longitudinal plasma wave theory, for propagation parallel and perpendicular to a magnetic field. This offers a very strong case for the validity of the Boltzmann equation approach. If it is accepted, then macroscopic and cold plasma theory follow automatically as progressively coarser approximations. As the ion acoustic wave results, and the observations of Tonks-Dattner resonances demonstrate, there are certainly experimental situations in which macroscopic theory is capable of predicting effects reasonably well which disappear when cold plasma theory is employed. Similarly, there are effects such as transverse wave propagation in the ordinary, extraordinary, and left-hand polarized modes, and longitudinal wave propagation in transmission line modes, for which cold plasma theory is generally adequate. Within the limits of this paper, the microscopic theory is essential only in the consideration of Landau and cyclotron damping, and cyclotron harmonic wave propagation.

Although longitudinal wave theory seems to be on very firm experimental foundations, the situation is rather less satisfactory for transverse waves. The success of the microscopic longitudinal wave theory suggests strongly that the microscopic transverse wave theory will be equally valid, but it would be reassuring to see more precise measurements on such effects as whistler propagation and attenuation due to cyclotron damping, and to see further extensions to the work on transverse wave propagation perpendicular to the magnetic field. The main obstacles are experimental. It is difficult to satisfy all of the requirements of the plane wave theory in the laboratory, and in any case, the temperature effects predicted are often small; for example, narrow windows in which absorption, or highly dispersive propagation, might be observed.

In this connection, it is important to remember that we have limited our discussion to laboratory experiments. We should not forget the plasma "laboratory" offered by space. Many of the modes most difficult to study experimentally in the laboratory, e.g. whistlers, have long been observed, understood, and even used for refined diagnostics in the ionosphere, the magnetosphere and beyond. It may well be that some of the more difficult verifications of fundamental plasma wave dispersion relations can best be carried out in space.

When the best laboratory plasma wave data are assembled, and compared with theory, they already present an encouraging picture. It is appropriate for us to consider what future progress remains to be made. The number of experimental situations and variables that might be taken into account is clearly limitless. From the point of view of the theoretician, further extensions are only useful if they give deeper insight into the application of the three simplified models of plasma behavior described in Section 2. For example, once the plane wave theory has been established, and one bounded system has been treated thoroughly, variations on the geometry may add very little to our basic understanding. Even so, there are many fundamental points which still remain to be cleared up. For example, the boundary conditions appropriate to plasmas confined by magnetic fields, dielectrics, and conducting walls, have still not all been discussed and measured precisely, and can greatly influence wave excitation and propagation. Detailed study of collisional effects and the Fokker-Planck equation would be valuable.

A similar point of view might be taken concerning charged particle velocity distributions. It might be argued that since microscopic theory seems to be appropriate for Maxwellian plasmas, then measurements on non-Maxwellian plasmas, where unstable waves can be predicted, are unnecessary. It is, perhaps, better to view this in the other sense: the "experiments" are already with us in common laboratory plasmas, nuclear fusion study machines, and in space plasmas. Instabilities are ubiquitous. Their classification and understanding can only be promoted by further study of the relevant dispersion relations, and refined laboratory experiments.

This reference to unstable waves leads us to the question of nonlinear plasma behavior. It was emphasized in Section 2 that plasma wave theory is founded on the small-signal approximation. Although there are some special theoretical solutions for large-amplitude waves, their stability has been questioned, and there do not seem to be experimental observations of them. If, in a given situation, there is wave growth, or a strong signal is applied to the plasma, then nonlinear effects are to be expected. These will couple modes together, and lead to energy transfer among them. It seems to the author that it is in this area that the next major thrust will be made by plasma wave experimentalists. From the theoretical point of view, the interaction of two waves to produce a third is the simplest case to study, before going on to the more complicated situations of broad spectra of modes interacting in turbulent plasmas.

There is already a rapidly-growing literature on such wave/wave interaction. As usual, the theory is running ahead of experiment and it is important that refined experiments should be carried out, particularly with the aim of checking large-signal microscopic theory. As a fascinating example of what can be done, we may mention some recent work by Malmberg et al.[50] These authors have shown that the nonlinear mixing of two signals can lead to what is effectively a reversal of Landau damping. This is only one of many significant experiments which can now be approached, and analyzed with confidence, as a result of the successful laboratory verifications of small-signal plasma wave theory.

ACKNOWLEDGEMENT

This work was supported by the National Aeronautics and Space Administration.

REFERENCES

1. J. A. Ratcliffe, The Magneto-ionic Theory and Its Application to the Ionosphere (University Press, Cambridge, 1959).

2. K. G. Budden, Radio Waves in the Ionosphere (University Press, Cambridge, 1961).

3. T. H. Stix, The Theory of Plasma Waves (McGraw-Hill, New York, 1962).

4. W. P. Allis, S. J. Buchsbaum and A. Bers, Waves in Anisotropic Plasmas (MIT Press, Cambridge, Mass., 1963).

5. J. J. Brandstatter, An Introduction to Waves, Rays and Radiation in Plasma Media (McGraw-Hill, New York, 1963).

6. J. F. Denisse and J. L. Delcroix, Plasma Waves (Interscience, New York, 1963).

7. V. L. Ginzburg, Propagation of Electromagnetic Waves in Plasmas (Pergamon, New York, 1964).

8. M. A. Heald, and C. B. Wharton, Plasma Diagnostics with Microwaves (John Wiley, New York, 1965).

9. I. P. Shkarofsky, T. W. Johnston and M. P. Bachynski, Particle Kinetics of Plasma (Addison-Wesley, Reading, Mass., 1965).

10. G. Bekefi, Radiation Processes in Plasmas (John Wiley, New York, 1966).

11. A. W. Trivelpiece, Slow-Wave Propagation in Plasma Waveguides (San Francisco Press, San Francisco, 1967).

12. J. R. Wait, Electromagnetics and Plasmas (Holt, Rinehart and Winston, New York, 1968).

13. R. J. Briggs, Electron-Stream Interaction with Plasmas (MIT Press, Cambridge, Mass., 1964).

14. J. A. Tataronis and F. W. Crawford (Proceedings of this Conference).

15. D. E. Baldwin and G. Rowlands, Phys. Fluids 9 (1966) 2444.

16. B. D. Fried, and S. D. Conte, The Plasma Dispersion Function (Academic Press, New York, 1961).

17. H. Derfler, Proc. VIIIth Int. Conf. on Phenomena in Ionized Gases, Vienna, Austria (in press).

18. E. B. Meservey, and S. P. Schlesinger, Phys. Fluids 8 (1965) 500.

19. T. Consoli and M. Dagai, J. Nucl. Eng. Pt. C 3 (1961) 115.

20. M. P. Bachynski, and B. W. Gibbs, Phys. Fluids 9 (1966) 532.

21. M. P. Bachynski, and B. W. Gibbs, Phys. Fluids 9 (1966) 520.

22. D. C. Mahaffey, Phys. Rev. 129 (1963) 1481.

23. D. E. Baldwin, D. M. Henderson, and J. L. Hirshfield, Phys. Rev. Letters 20 (1968) 314.

24. A. W. Trivelpiece and R. W. Gould, J. Appl. Phys. 30 (1959) 1784.

25. H. L. Stover, Stanford University Microwave Laboratory Report No. 1140 (1964).

26. J. H. Malmberg, and C. B. Wharton, Phys. Rev. Letters 13 (1964) 184.

27. J. H. Malmberg, C. B. Wharton, and W. E. Drummond, Proc. Conf. on Plasma Phys. and Controlled Fusion, Culham, England, 1965 (IAEA, 1966) Vol. 1, 485.

28. J. H. Malmberg, and C. B. Wharton, Phys. Rev. Letters 17 (1966) 175.

29. G. van Hoven, Phys. Rev. Letters 17 (1966) 169.

30. H. Derfler and T. C. Simonen, Phys. Rev. Letters 17 (1966) 172.

31. H. Derfler and T. C. Simonen, J. Appl. Phys. 38 (1967) 5014.

32. H. J. Schmitt, Appl. Phys. Letters 4,(1964) 111.

33. H. J. Schmitt, G. Meltz, and P. J. Freyheit, Phys. Rev. 139 (1965) A1432.

34. J. V. Parker, J. C. Nickel, and R. W. Gould, Phys. Fluids 7 (1964) 1489.

35. F. W. Crawford, Phys. Letters 5 (1966) 244.

36. K. J. Harker, Phys. Fluids 11 (1968) 425.

37. W. D. Jones and I. Alexeff, Proc. VIIth Int. Conf. on Phenomena in Ionized Gases, Belgrade, Yugoslavia, 1965 (Gradevinska Knjiga Pub., Belgrade, 1966) Vol. 2, 330.

38. B. D. Fried and R. W. Gould, Phys. Fluids 4 (1961) 139.

39. A. T. Wong, N. D'Angelo and R. W. Motley, Phys. Rev. Letters 9 (1962) 415.

40. P. J. Barrett and P. F. Little, Phys. Rev. Letters, 14 (1965) 356.

41. L. C. Woods, J. Fluid Mech. 23 (1965) 315.

42. F. W. Crawford, and S. A. Self, Proc. VIth Int. Conf. on Ionization Phenomena in Gases, Paris, France, 1963 (SERMA, Paris 1964) Vol. 3, 51.

43. F. W. Crawford, H. N. Ewald and S. A. Self, Stanford University Institute for Plasma Research Report No. 229 (1968).

44. R. S. Harp, Proc. VII Int. Conf. on Phenomena in Ionized Gases, Belgrade, Yugoslavia, 1965 (Gradevinska Knjiga Pub., Belgrade, 1966) Vol. 2, 294.

45. T. D. Mantei, Stanford University Institute for Plasma Research Report No. 194 (1967).

46. F. W. Crawford, R. S. Harp, and T. D. Mantei, Phys. Rev. Letters 17 (1966) 626.

47. F. W. Crawford, R. S. Harp, and T. D. Mantei, J. Geophys. Res. 72 (1967) 57.

48. S. J. Buchsbaum and A. A. Hasegawa, Phys. Rev. Letters 12 (1964) 685.

49. S. J. Buchsbaum and A. A. Hasegawa, Phys. Rev. 143 (1966) 303.

50. J. H. Malmberg, C. B. Wharton, R. W. Gould, and T. M. O'Neill, Phys. Rev. Letters 20 (1968) 95.

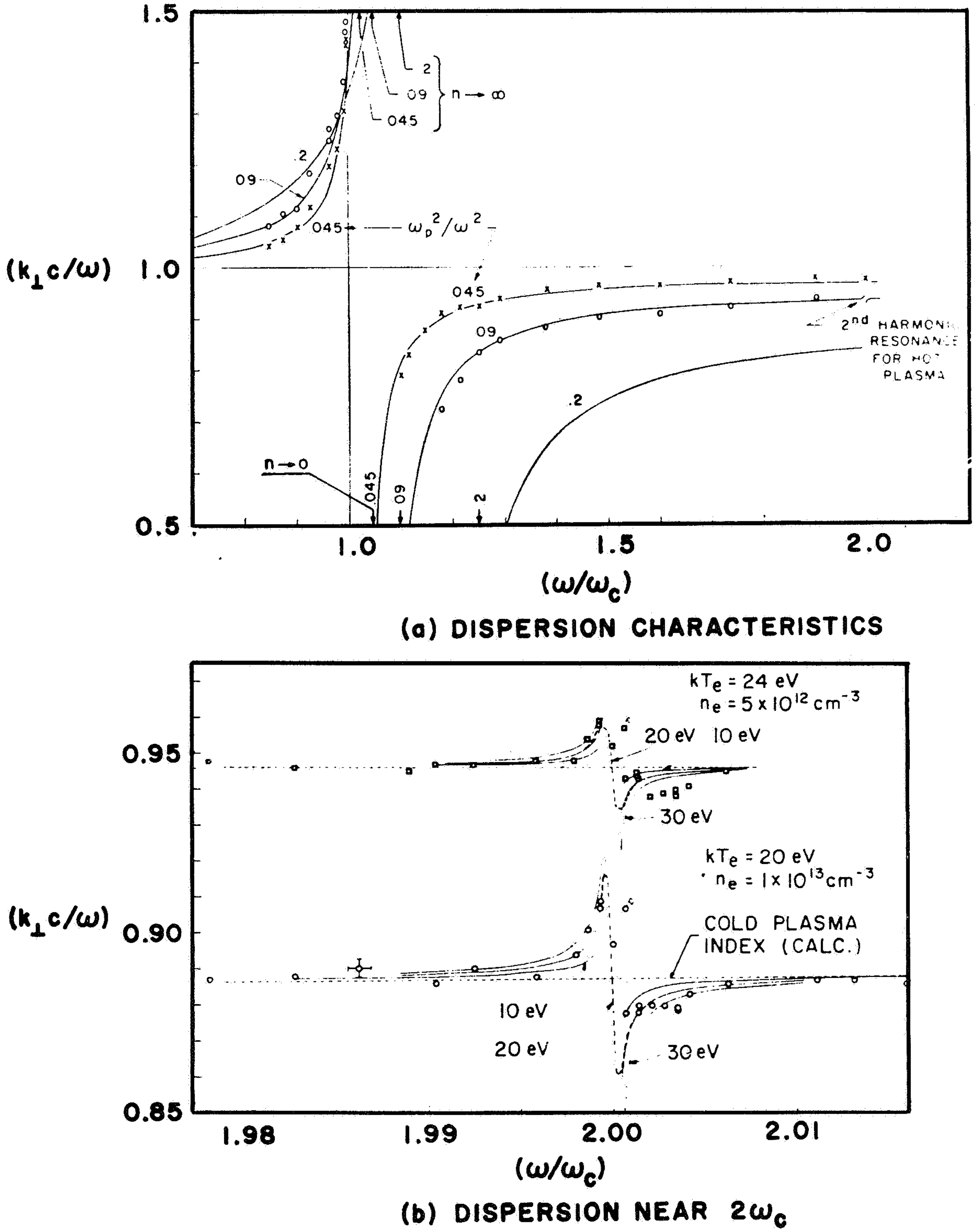

FIG. 1. TRANSVERSE WAVE PROPAGATION: $\underset{\sim}{E} \perp \underset{\sim}{B}_0$, $\underset{\sim}{k} \perp \underset{\sim}{B}_0$ (after Meservey and Schlesinger).

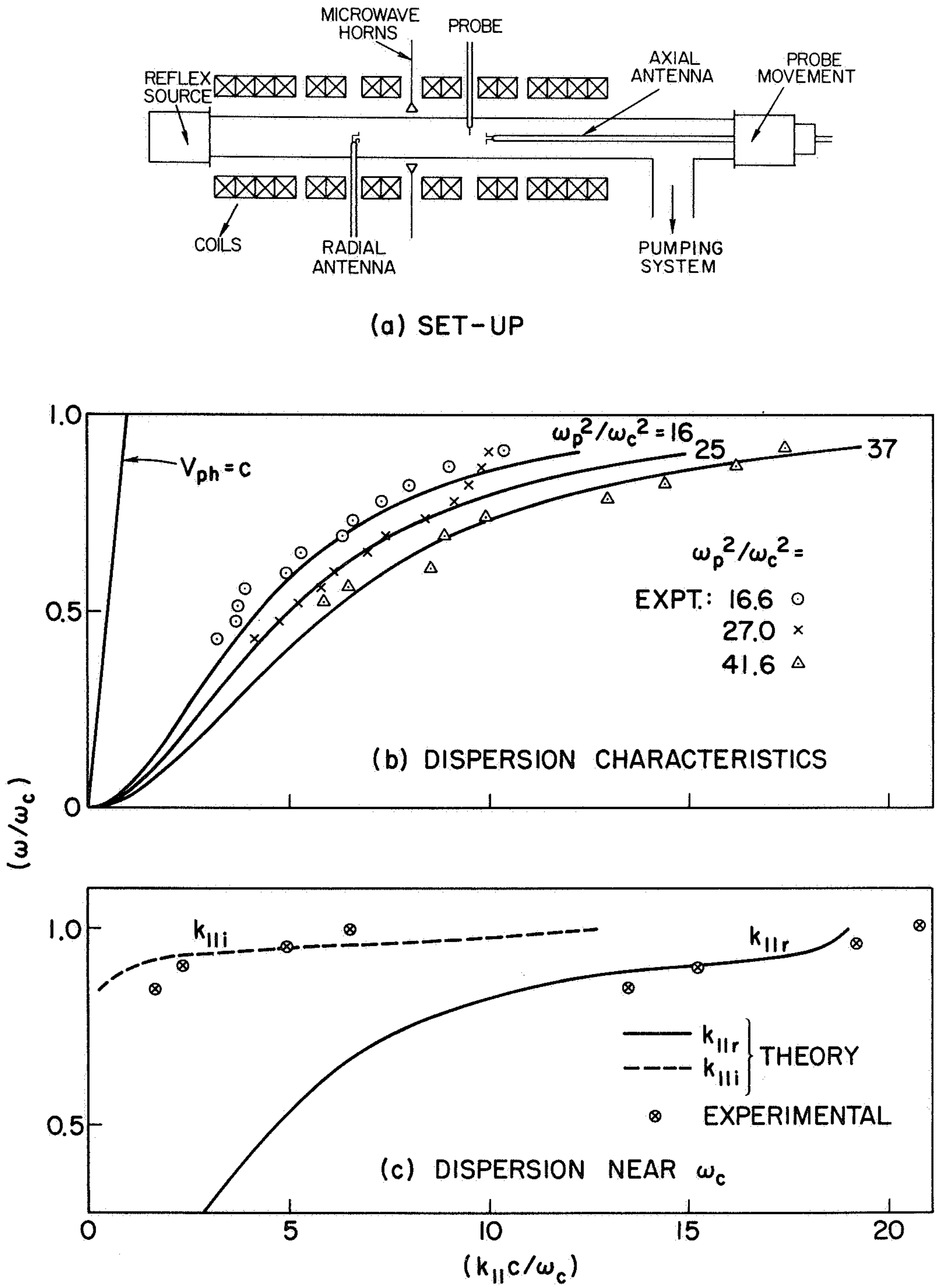

FIG. 2. TRANSVERSE WAVE PROPAGATION: $\underset{\sim}{E} \perp \underset{\sim}{B}_0$, $\underset{\sim}{k} \parallel \underset{\sim}{B}_0$ (Crawford, Fessenden, and Lee, unpublished work).

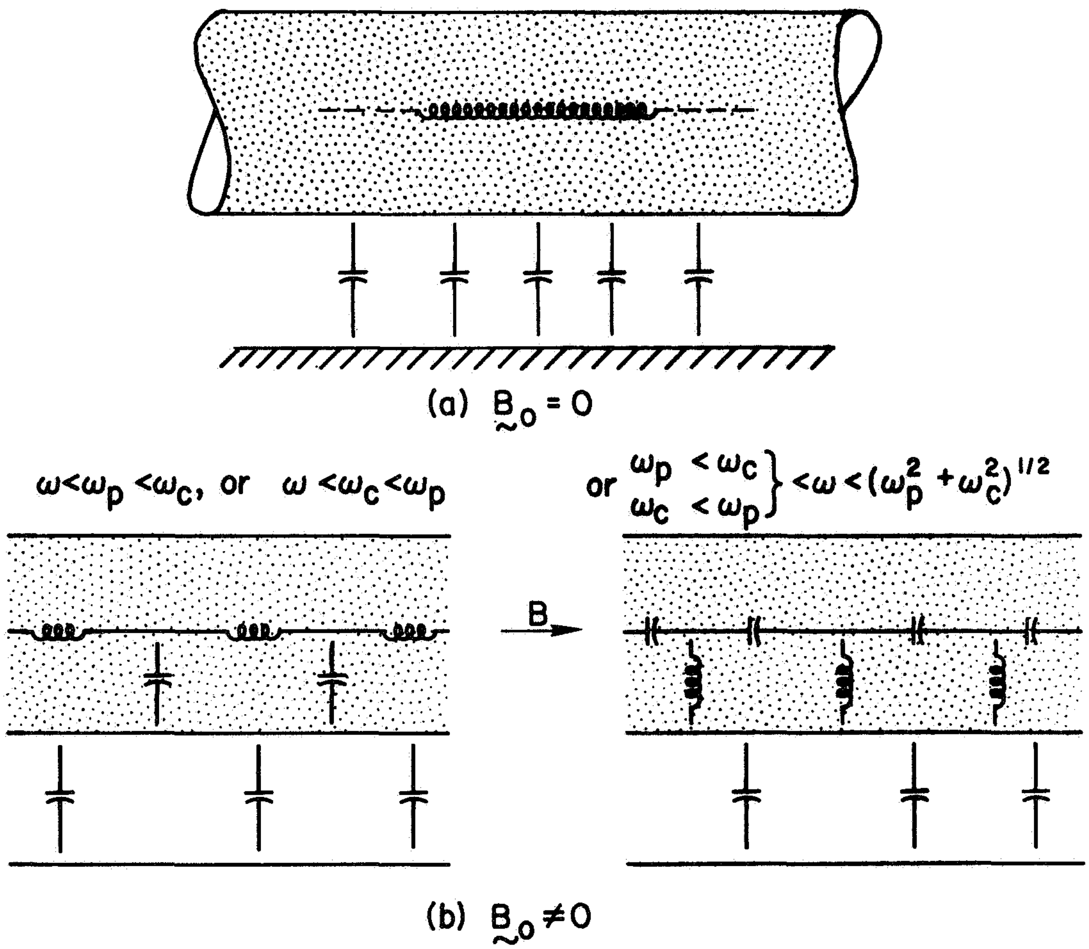

FIG. 3. TRANSMISSION LINE MODES: CIRCUIT ANALOGS.

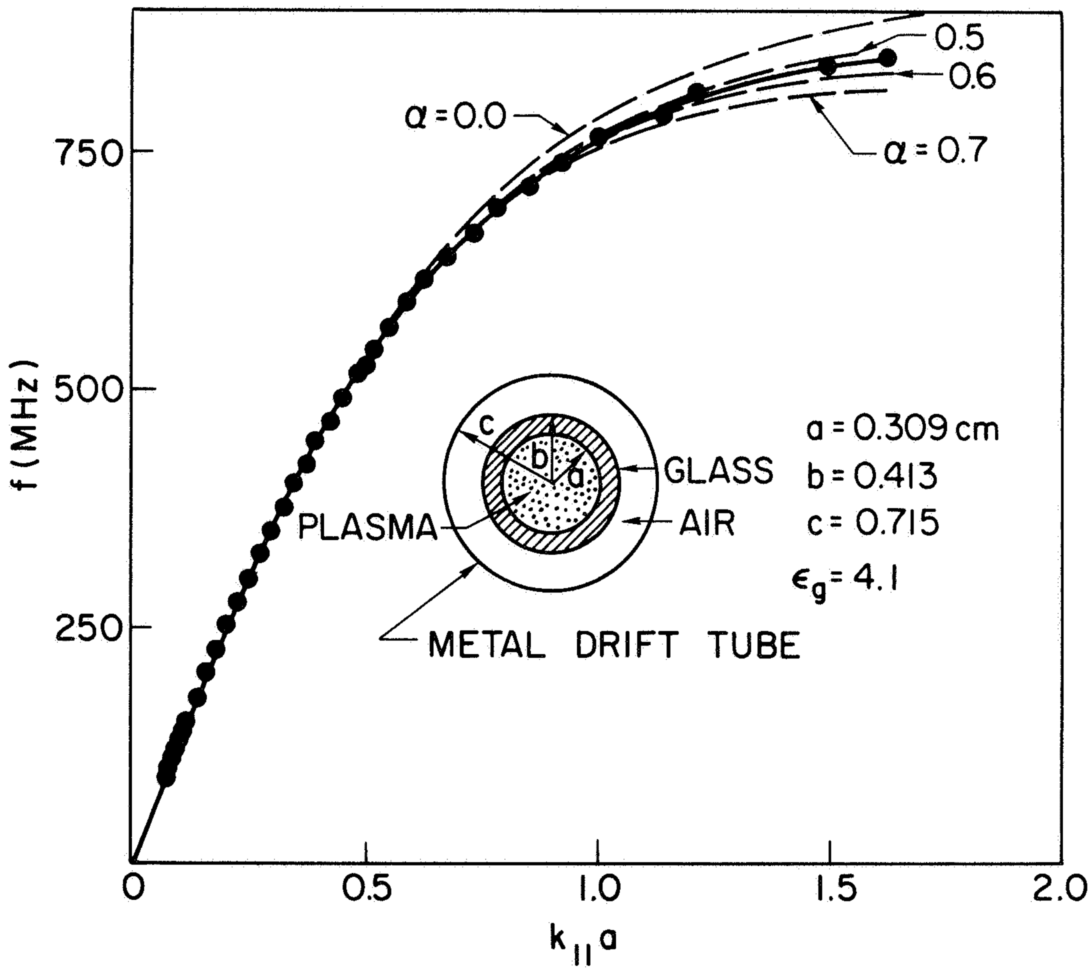

(a) $\underset{\sim}{B}_0 = 0$ (AFTER STOVER)

FIG. 4. TRANSMISSION LINE MODES: EXPERIMENTAL RESULTS.

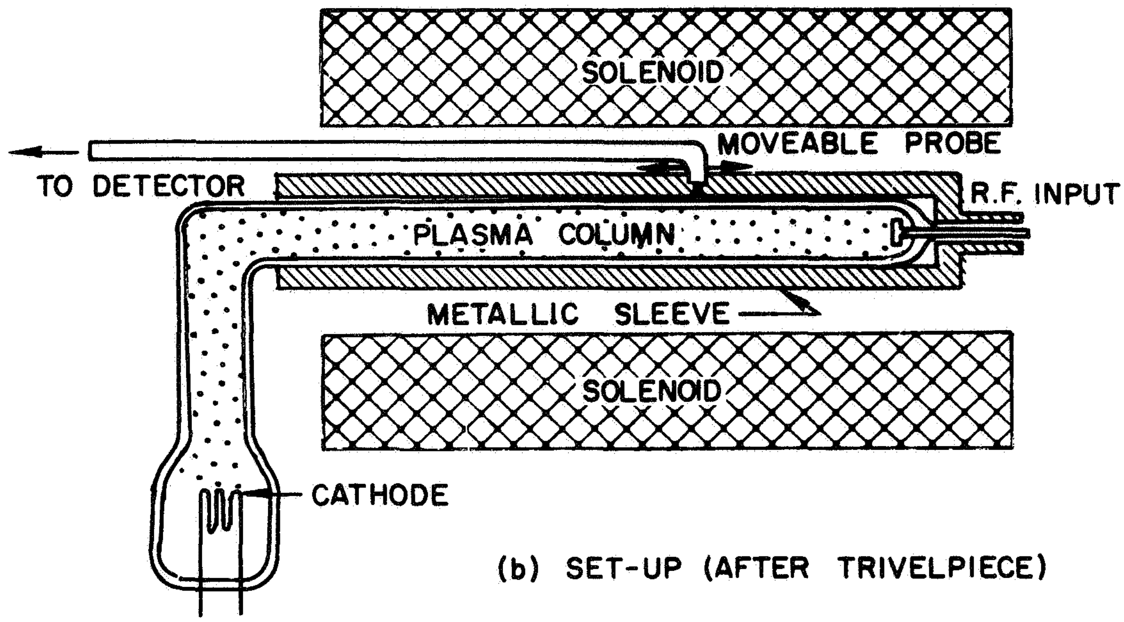

(b) SET-UP (AFTER TRIVELPIECE)

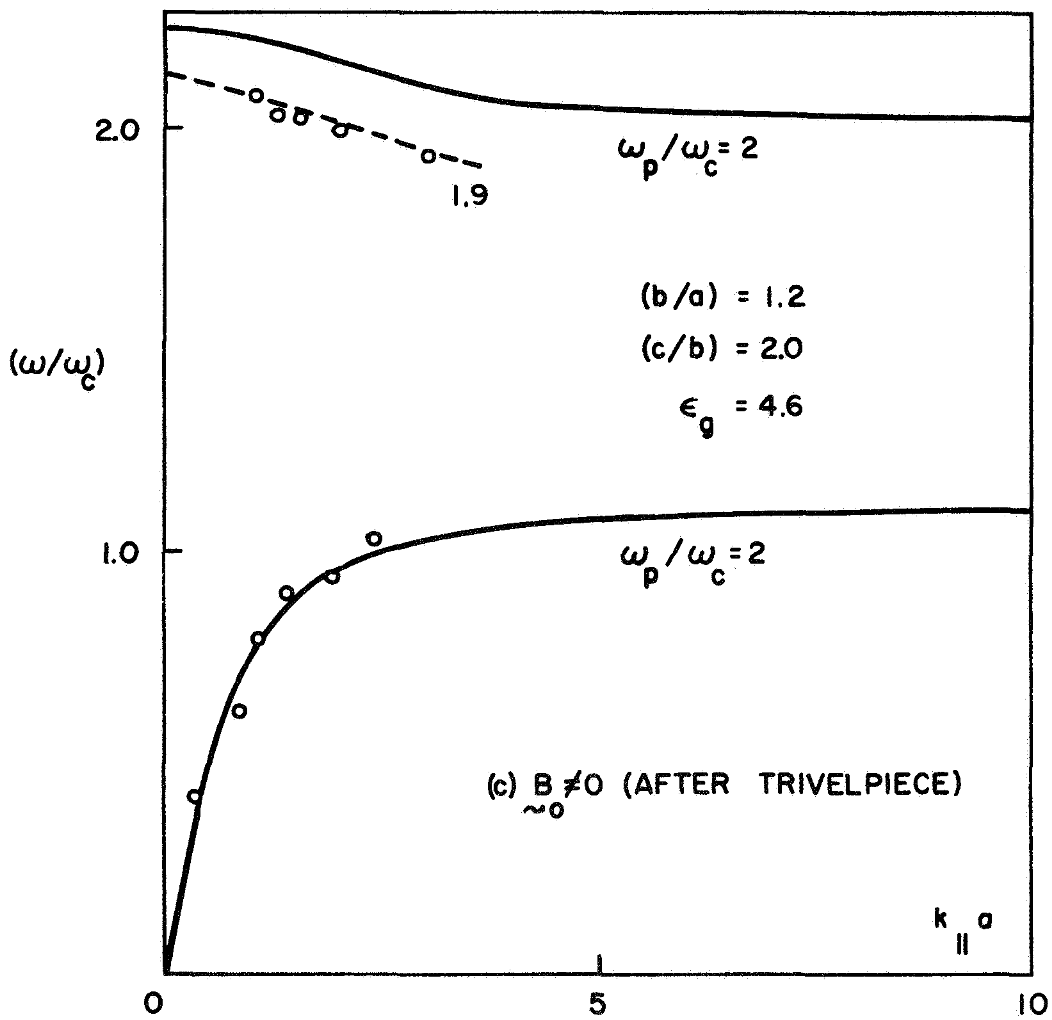

(c) $B_0 \neq 0$ (AFTER TRIVELPIECE)

FIG. 4. CONTINUED

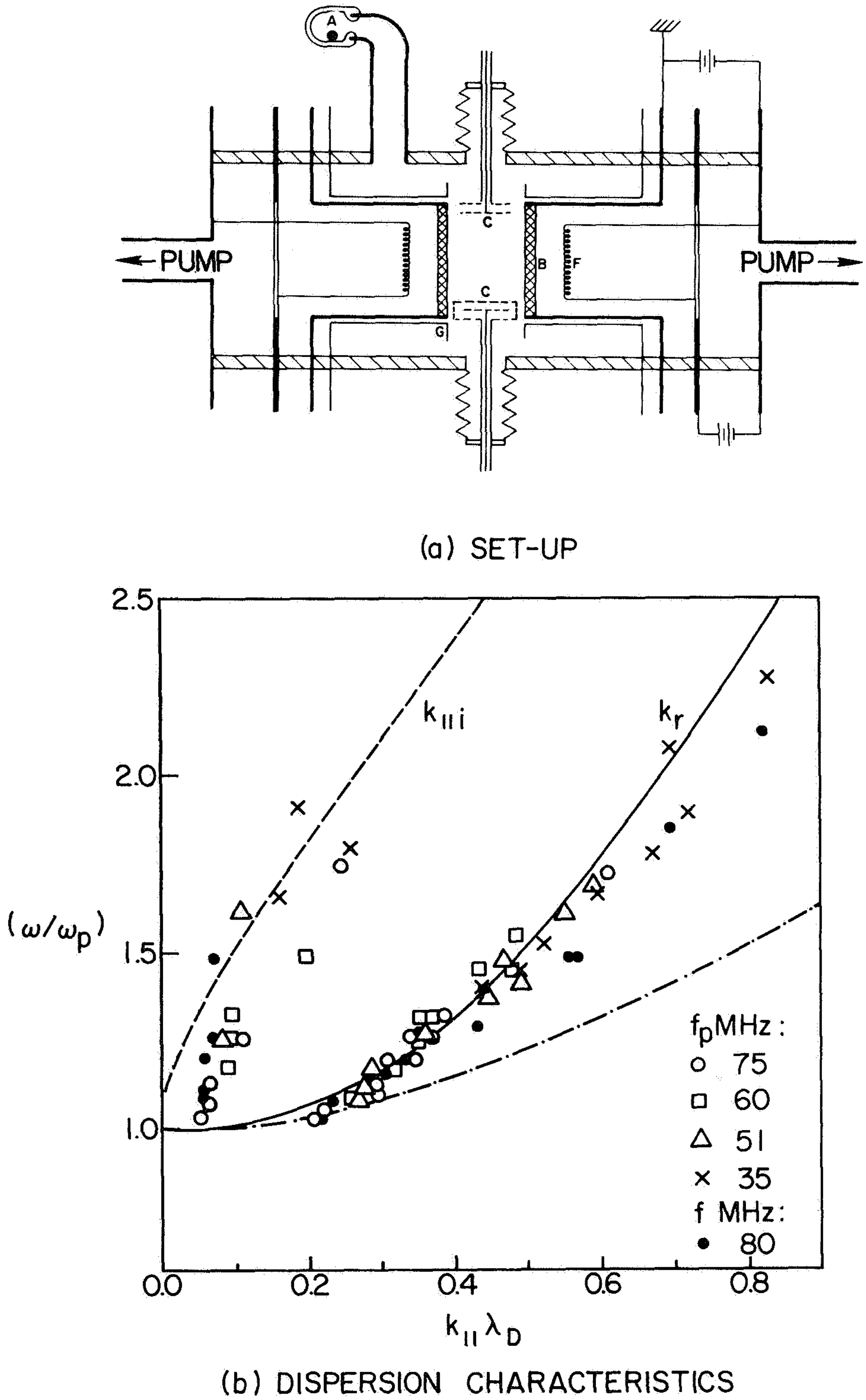

FIG. 5. LONGITUDINAL WAVE PROPAGATION: $\underset{\sim}{E} \parallel \underset{\sim}{B}_0$, $\underset{\sim}{k} \parallel \underset{\sim}{B}_0$ (after Derfler and Simonen).

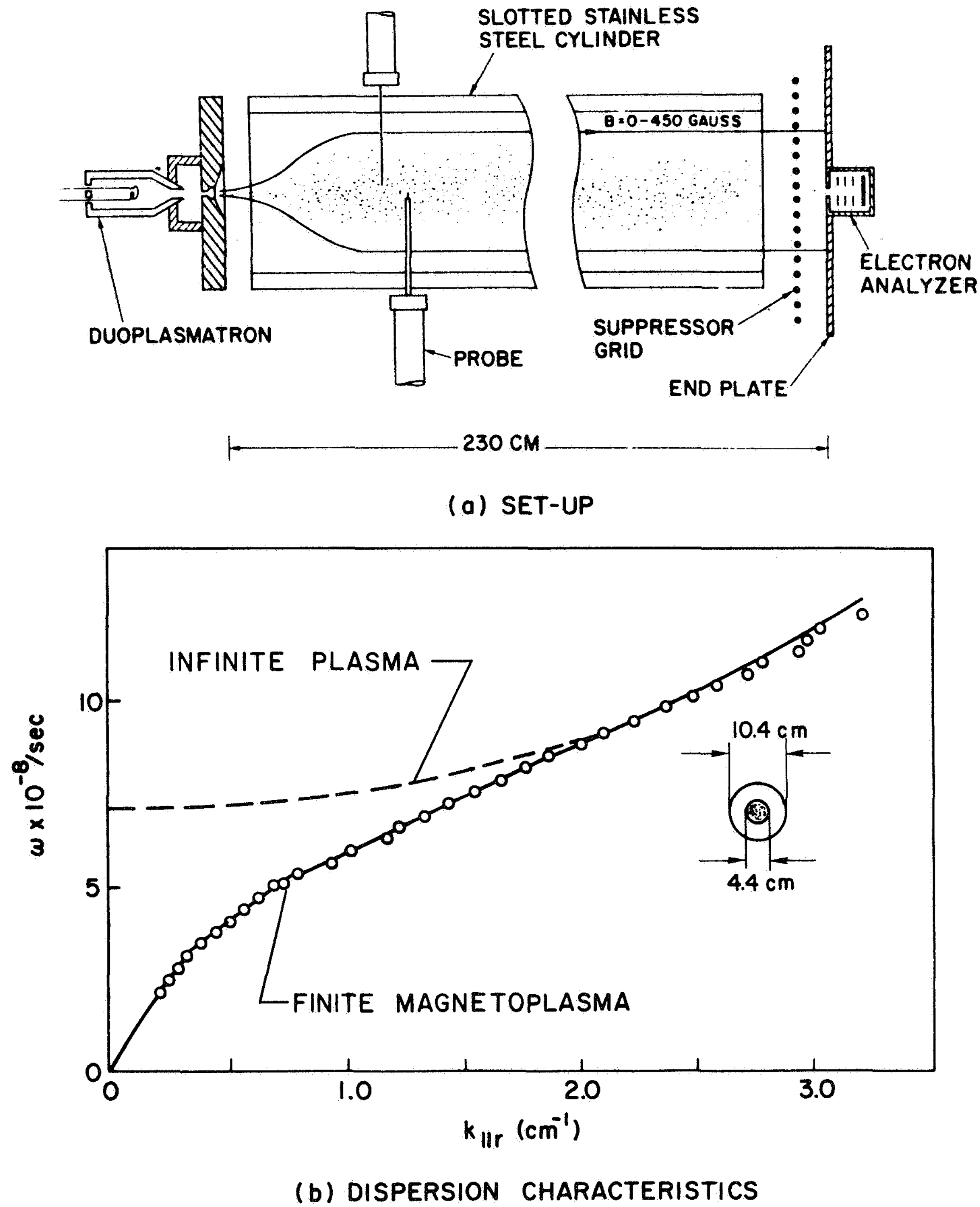

FIG. 6. LONGITUDINAL WAVE PROPAGATION IN A BOUNDED PLASMA: $\underset{\sim}{E} \parallel \underset{\sim}{k}$ (after Malmberg and Wharton).

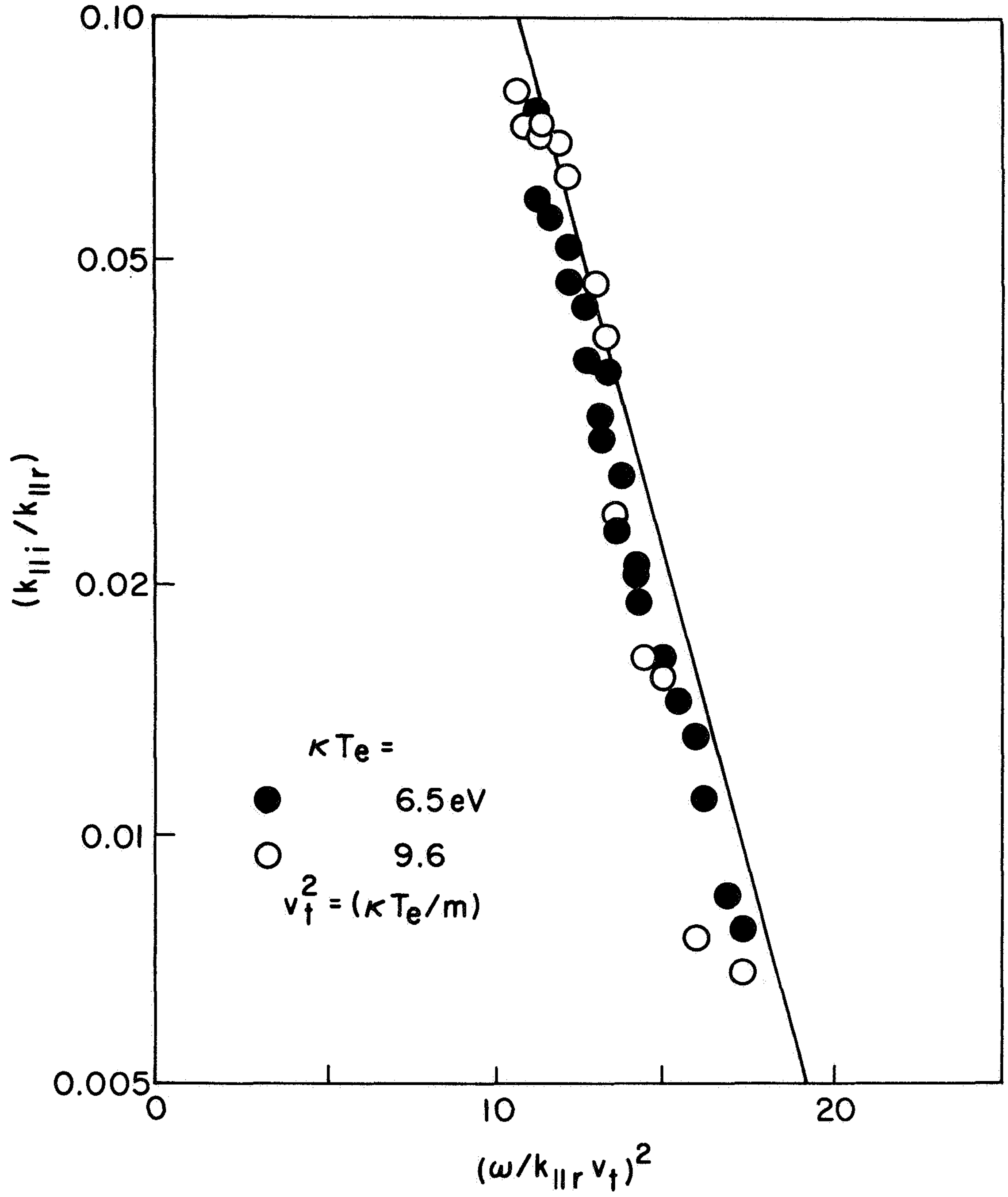

(c) ATTENUATION

FIG. 6. CONTINUED

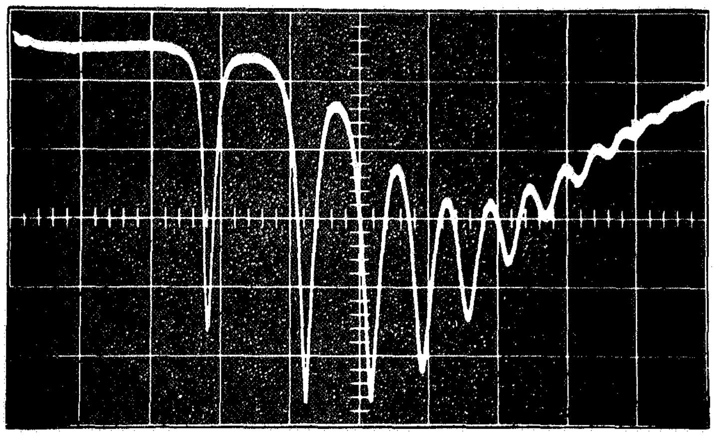

(a) RESONANCES (after Schmitt et al)

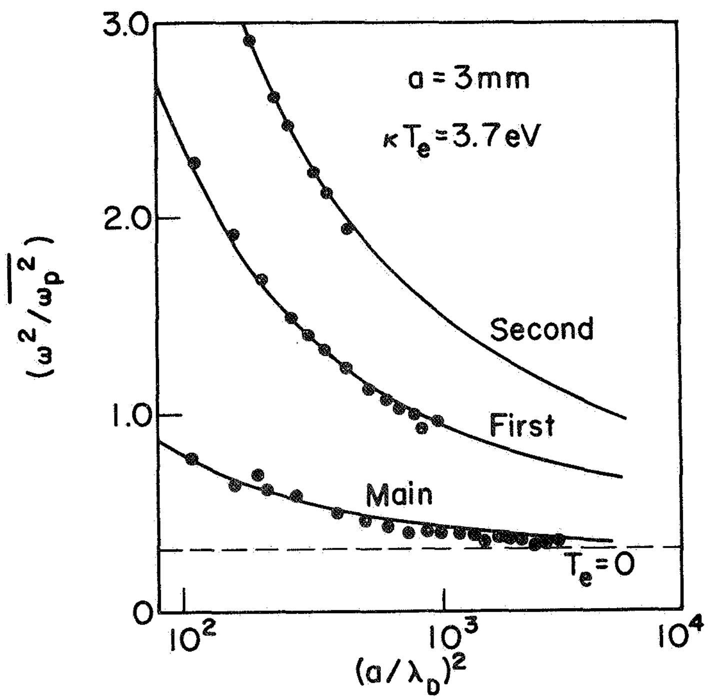

(b) LOCATION OF PEAKS (after Parker et al)

FIG. 7. LONGITUDINAL WAVE PROPAGATION IN A BOUNDED PLASMA: TONKS-DATTNER RESONANCES.

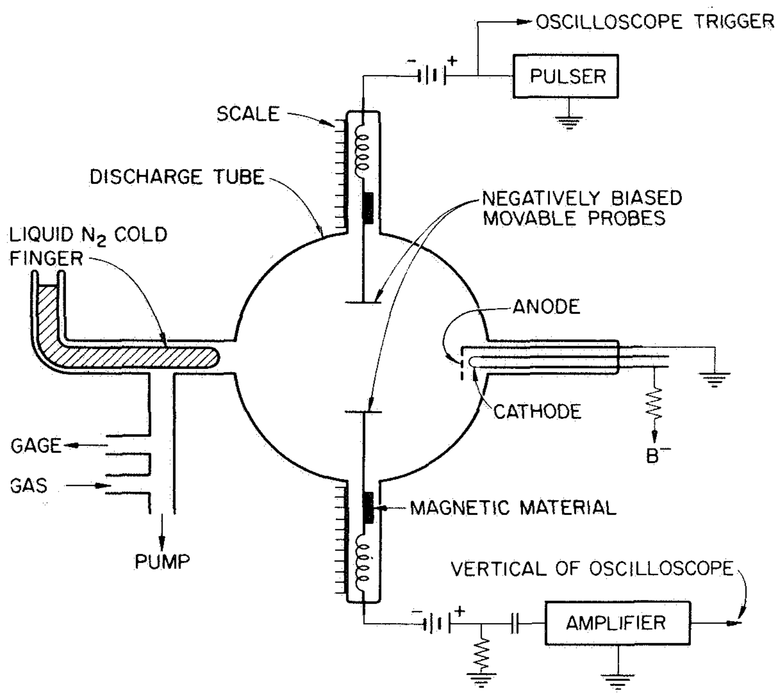

(a) SET-UP

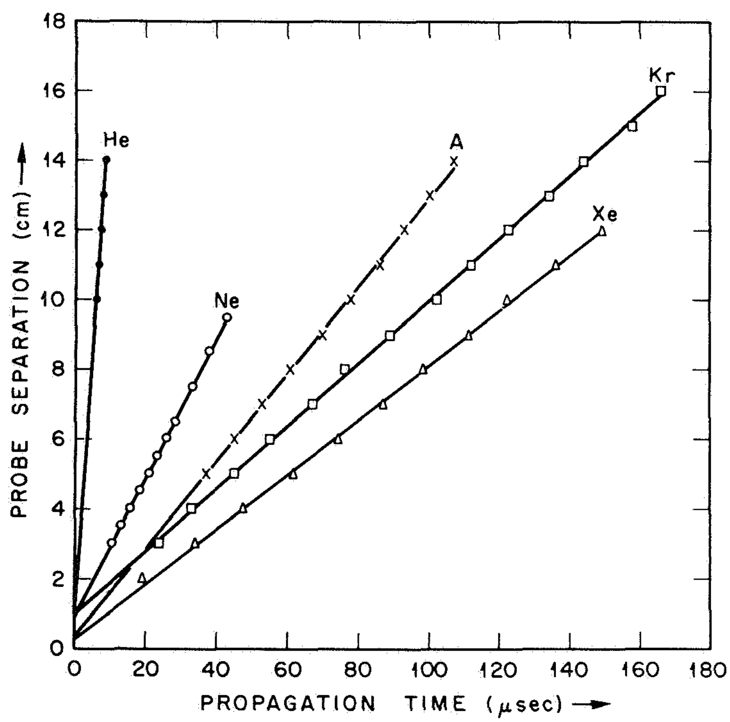

(b) TIME OF FLIGHT

FIG. 8. LONGITUDINAL WAVE PROPAGATION: ION ACOUSTIC WAVES ($T_e \gg T_i$) (after Jones and Alexeff).

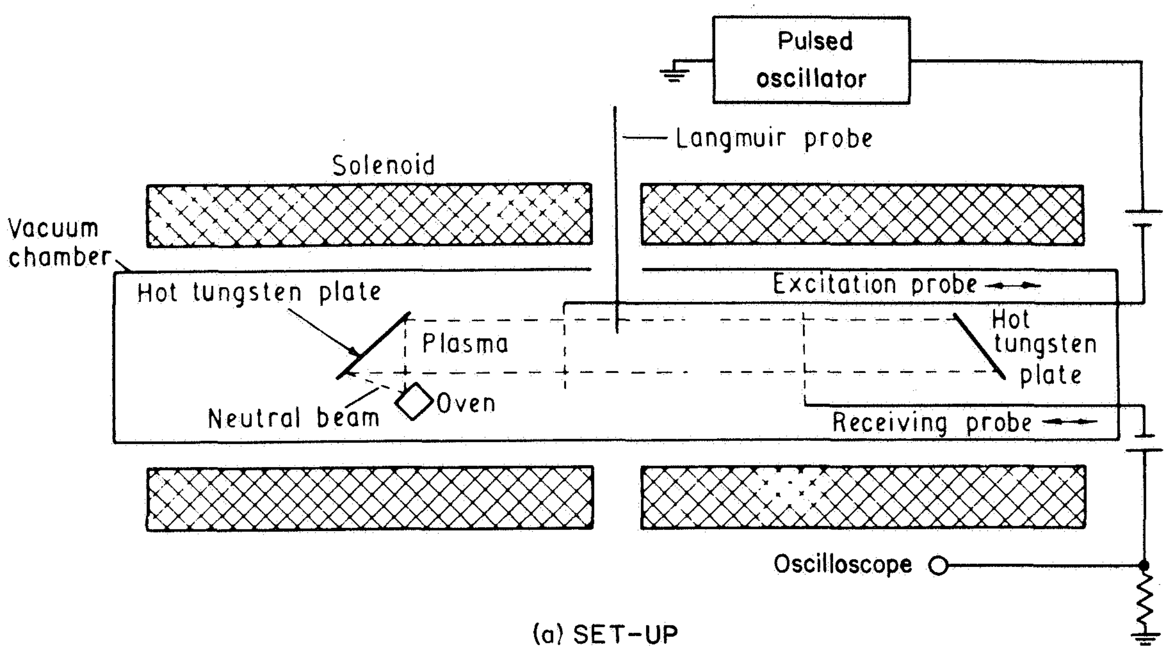

(a) SET-UP

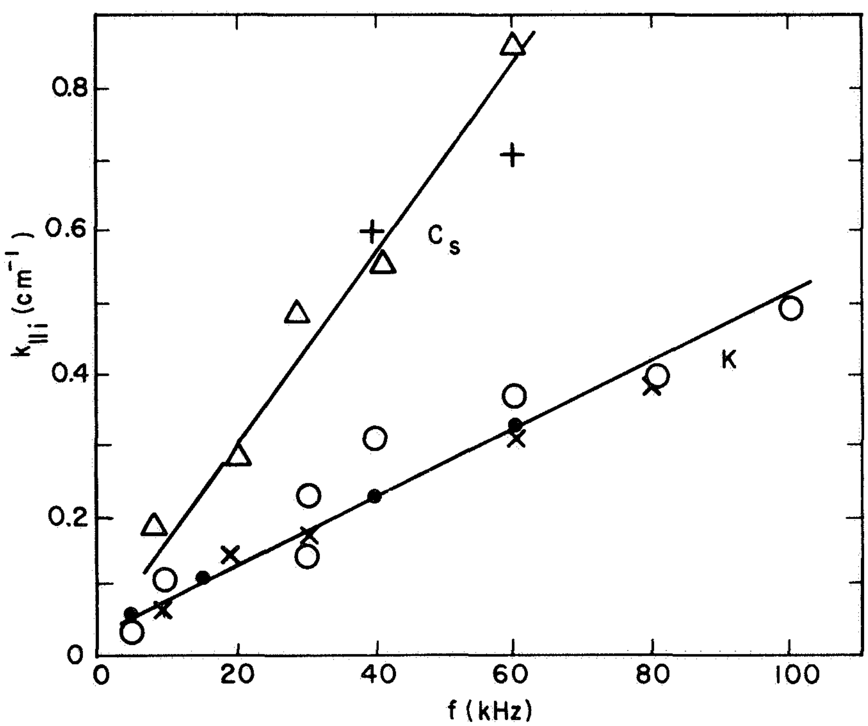

(b) ATTENUATION

FIG. 9. LONGITUDINAL WAVE PROPAGATION: ION ACOUSTIC WAVES ($T_e \approx T_i$) (after Wong et al).

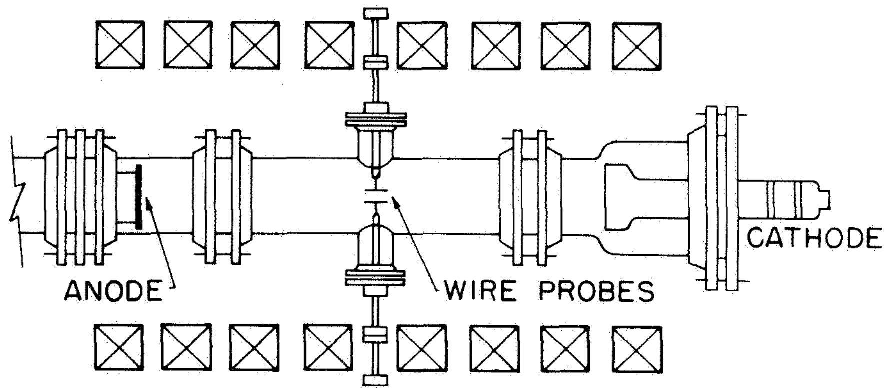

(a) SET-UP

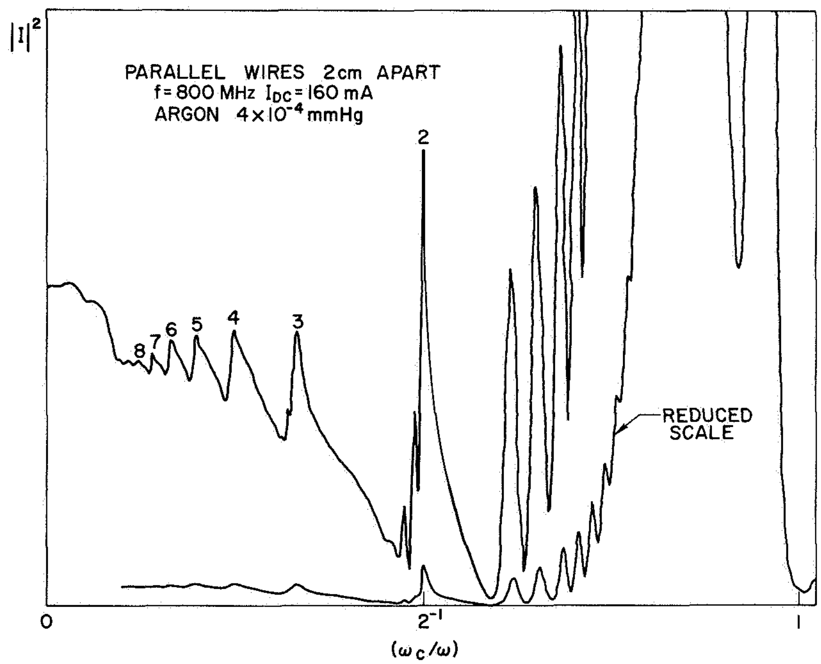

(b) TYPICAL RECORD

FIG. 10. LONGITUDINAL WAVE PROPAGATION: $\underset{\sim}{E} \perp \underset{\sim}{B}_0$, $\underset{\sim}{k} \perp \underset{\sim}{B}_0$ (after Mantei).

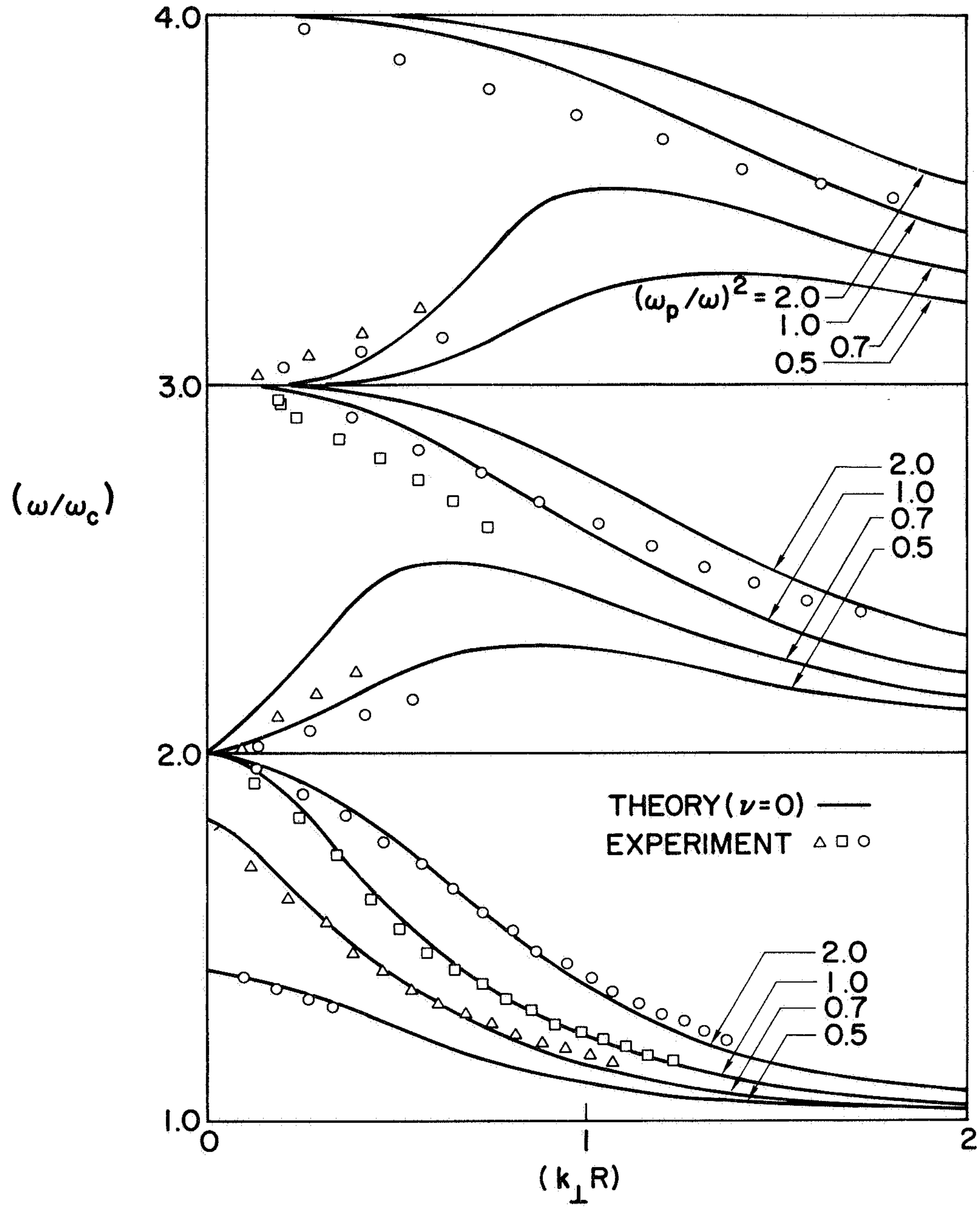

(c) DISPERSION CHARACTERISTICS

FIG. 10. CONTINUED

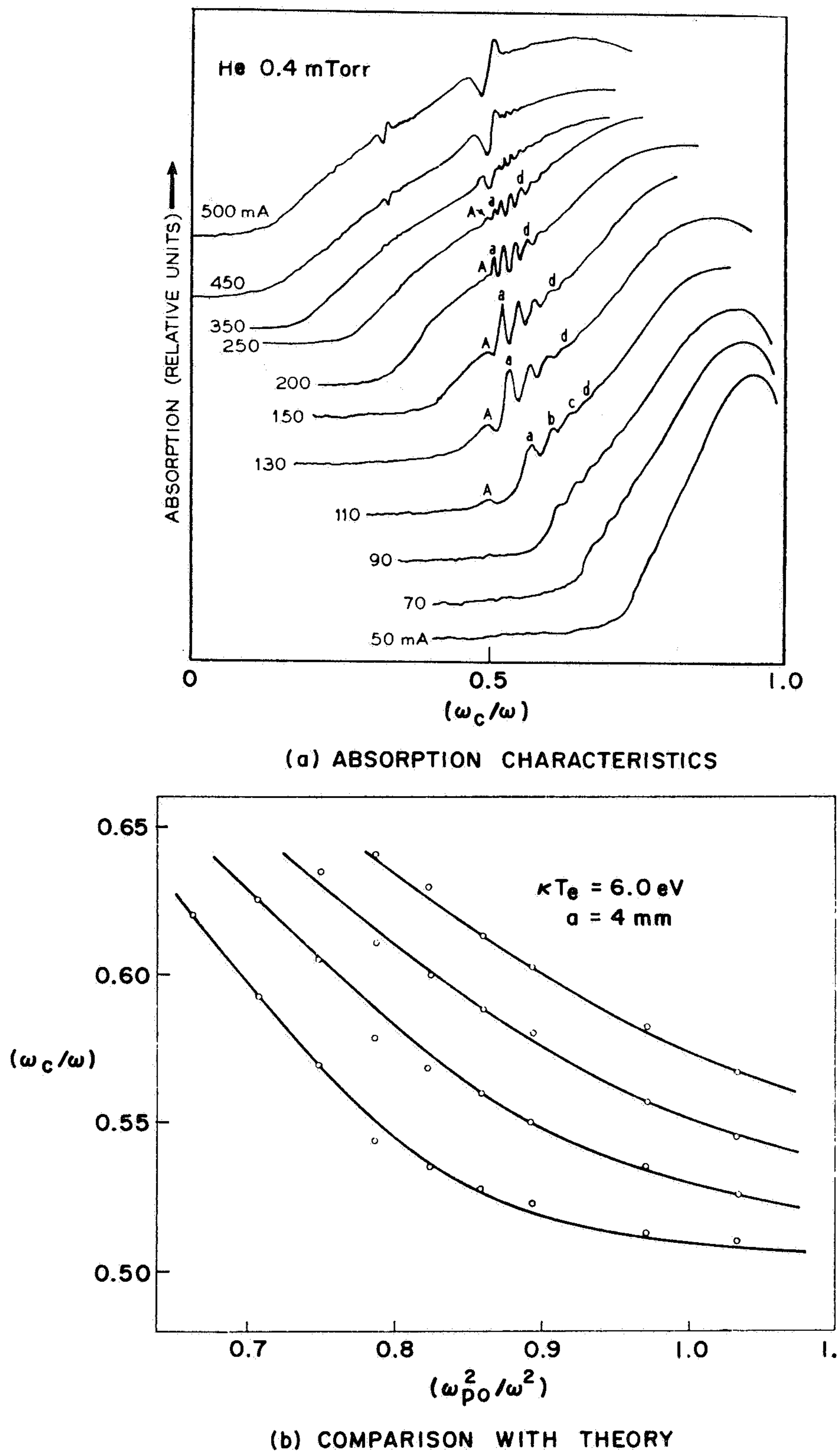

FIG. 11. LONGITUDINAL WAVE PROPAGATION IN A BOUNDED PLASMA $\underset{\sim}{E} \perp \underset{\sim}{B}_0$, $\underset{\sim}{k} \perp \underset{\sim}{B}_0$ (after Buchsbaum and Hasegawa).